Tree Growth Enhancement Drives a Persistent Biomass Gain in Unmanaged Temperate Forests

Author(s):
Marqués, Laura; Weng, Ensheng; Bugmann, Harald; Forrester, David I.; Rohner, Brigitte; Hobi, Martina L.; Trotsiuk, Volodymyr; Stocker, Benjamin

Publication date:
2023-10

Permanent link:
https://doi.org/10.3929/ethz-b-000639049

Originally published in:
AGU Advances 4(5), https://doi.org/10.1029/2022AV000859

Funding acknowledgement:
181115 - next-generation Modelling of the biosphere - Including New Data streams and optimality approaches (SNF)

AGU ADVANCING EARTH AND SPACE SCIENCES

AGU Advances

RESEARCH ARTICLE
10.1029/2022AV000859

Peer Review The peer review history for this article is available as a PDF in the Supporting Information.

Key Points:

- Observations from unmanaged forests in Switzerland suggest a temporal and spatial trend toward higher tree densities per unit of tree size
- Simulated tree growth enhancements lead to biomass increments despite reductions in tree longevity—consistent with observed trends
- These results reconcile reports of tree longevity reductions with model predictions of persistent biomass increases

Supporting Information:

Supporting Information may be found in the online version of this article.

Correspondence to:

L. Marqués,
laura.marques@unibe.ch

Citation:

Marqués, L., Weng, E., Bugmann, H., Forrester, D. I., Rohner, B., Hobi, M. L., et al. (2023). Tree growth enhancement drives a persistent biomass gain in unmanaged temperate forests. *AGU Advances*, *4*, e2022AV000859. https://doi.org/10.1029/2022AV000859

Received 9 DEC 2022
Accepted 5 SEP 2023

Author Contributions:

Conceptualization: Laura Marqués, Benjamin D. Stocker
Data curation: Laura Marqués
Formal analysis: Laura Marqués, Ensheng Weng, Benjamin D. Stocker
Funding acquisition: Benjamin D. Stocker
Investigation: Harald Bugmann, David I. Forrester, Brigitte Rohner, Martina L. Hobi, Volodymyr Trotsiuk

Tree Growth Enhancement Drives a Persistent Biomass Gain in Unmanaged Temperate Forests

Laura Marqués[1,2,3,4], Ensheng Weng[5], Harald Bugmann[6], David I. Forrester[2,7], Brigitte Rohner[2], Martina L. Hobi[2], Volodymyr Trotsiuk[2], and Benjamin D. Stocker[1,2,3,4]

[1]Department for Environmental Systems Science, Institute of Agricultural Sciences, ETH Zurich, Zurich, Switzerland, [2]Swiss Federal Institute for Forest, Snow and Landscape Research WSL, Birmensdorf, Switzerland, [3]Institute of Geography, University of Bern, Bern, Switzerland, [4]Oeschger Centre for Climate Change Research, University of Bern, Bern, Switzerland, [5]Center for Climate Systems Research, NASA Goddard Institute for Space Studies, Columbia University, New York, NY, USA, [6]Department of Environmental Systems Science, Forest Ecology, Institute of Terrestrial Ecosystems, ETH Zurich, Zurich, Switzerland, [7]CSIRO Environment, Canberra, ACT, Australia

Abstract While enhanced tree growth over the last decades has been reported in forests across the globe, it remains unclear whether it drives persistent biomass increases of forest stands, particularly in mature forests. Enhanced tree growth and stand-level biomass are often linked with a simultaneous increase in density-driven mortality and a reduction in tree longevity. Identifying empirical evidence regarding the balance between these processes is challenging due to the confounding effects of stand history, management, and environmental changes. Here, we investigate the link between growth and biomass via the negative relationship between average tree size and stand density (tree number per area). We find increasing stand density for a given mean tree size in unmanaged closed-canopy forests in Switzerland over the past six decades and a positive relationship between tree growth and stand density across forest plots—qualitatively consistent with our simulations using a mechanistic, cohort-resolving ecosystem model (BiomeE). Model simulations show that, in the absence of other disturbances, enhanced tree growth persistently increases biomass stocks despite simultaneous decreases in carbon residence time and tree longevity. However, the magnitude of simulated biomass changes for a given growth enhancement critically depends on the shape of the mortality functions. Our analyses reconcile reports of growth-induced reductions of tree longevity with model predictions of persistent biomass increases, and with our finding of trends toward denser forests in response to growth—also in mature stands.

Plain Language Summary Tree growth has increased globally over the last decades but the implications for long-term carbon storage in forests remain unknown. Tree growth enhancement could be translated into an increase in biomass or associated with a reduction in tree longevity compensating for any potential change in biomass. It has been difficult to study these processes because forests are commonly affected by past management and environmental changes. In this study, we investigate whether accelerated tree growth leads to increases in forest biomass by combining forest observations and a vegetation demography model. We find that unmanaged forests in Switzerland have been thickening over the past six decades. Model simulations agree with observations and show that, in the absence of other disturbances, enhanced tree growth persistently increases biomass stocks despite simultaneous decreases in carbon residence time and tree longevity. However, the magnitude of simulated changes critically depends on the mortality function in the model. Our analyses reconcile previous contrasting results of reductions of tree longevity with model predictions of biomass increases and with our finding of observed trends toward denser forests in response to growth.

1. Introduction

Forest demographic processes, namely growth, recruitment, and mortality, are being altered by global environmental change (McDowell et al., 2020). Enhanced tree growth over the last decades has been widely reported (Brienen et al., 2015; Cole et al., 2009; Fang et al., 2014; McMahon et al., 2010; Wu et al., 2014). Trends in forest stand growth have been attributed to increased nutrient inputs by atmospheric deposition, rising temperatures and extended growing seasons (Anderegg et al., 2015; Pretzsch et al., 2014), and elevated atmospheric carbon dioxide (eCO_2) (Huang et al., 2007; Hubau et al., 2020; Lewis et al., 2009; Phillips et al., 2009; Walker et al., 2019).

Methodology: Laura Marqués, Ensheng Weng, Benjamin D. Stocker
Resources: Harald Bugmann, David I. Forrester, Brigitte Rohner, Martina L. Hobi, Volodymyr Trotsiuk
Software: Ensheng Weng
Visualization: Laura Marqués
Writing – original draft: Laura Marqués, Benjamin D. Stocker
Writing – review & editing: Ensheng Weng, Harald Bugmann, David I. Forrester, Brigitte Rohner, Martina L. Hobi, Volodymyr Trotsiuk

Also, biomass stocks have been reported to have increased in forests around the globe (Pan et al., 2011), unless logging, large-scale disturbances, and extreme events reversed long-term trends (Wang et al., 2021). However, it remains unclear to what extent increased biomass stocks are a consequence of accelerated tree growth in response to environmental change or of recovery from past disturbances and land use (Frelich, 2002; Gloor et al., 2009). Disturbance history and stand age are dominant factors determining forest biomass stocks (Bradford et al., 2008) and can mask the effects of environmental change. This limits our understanding and poses an observational challenge for attributing the observed forest carbon (*C*) sink (Pan et al., 2011) to anthropogenic versus environmental drivers, and for answering the question of whether accelerated tree growth, induced by environmental change, leads to persistent increases in forest biomass stocks. Understanding the relationship between growth and biomass is thus key also for the role of CO_2 fertilization of photosynthesis and growth in driving the observed terrestrial *C* sink (Walker et al., 2021).

Direct evidence for environmental change effects on tree growth and biomass comes from ecosystem manipulation experiments. Free Air CO_2 Enrichment (FACE) experiments have identified increases in biomass production in response to enhanced CO_2 (Ainsworth & Long, 2005; Hovenden et al., 2019; Jiang et al., 2020; Norby et al., 2005; Walker et al., 2021). However, positive effects on biomass stocks have been argued to be transitory (Brienen et al., 2020; Bugmann & Bigler, 2011; Büntgen et al., 2019; Fatichi et al., 2019; Fleischer et al., 2019) without long-term increases in carbon storage (Körner, 2006, 2009), or limited to young forests (Norby & Zak, 2011). This argument can be linked to two hypothesized mechanisms. First, the *progressive nitrogen (N) limitation* hypothesis (Luo et al., 2004) states that soil *N* gets progressively depleted as biomass stocks accumulate. Old-growth forests are prone to *N* scarcity, reducing growth and triggering additional feedback via increases in the *C*:*N* ratio of litter and ensuing decreases in net mineralization rates. Second, the *grow-fast-die-young* hypothesis (hereafter GFDY) (Brienen et al., 2020; Bugmann & Bigler, 2011; Büntgen et al., 2019; Körner, 2017) posits a reduced longevity of fast-growing trees, as described in more detail below. Both hypotheses predict that a positive response of biomass stocks to enhanced tree growth would be reduced or fully suppressed in mature stands. Indeed, the first FACE experiment conducted in a mature stand did not show increased vegetation biomass carbon sequestration at the ecosystem level (Jiang et al., 2020), even if it is not fully established whether the observed response was due to forest demography or nutrient availability-related mechanisms (Ellsworth et al., 2017). Here, we investigate whether increased biomass production leads to persistent enhancements of biomass stocks, subject to the negative growth rate-longevity relationship suggested by the GFDY hypothesis. Since limiting effects by *N* scarcity (Norby et al., 2010), and nutrient-depleted soils in general (Vicca et al., 2012), act predominantly on biomass productivity and not directly on biomass stocks and their persistence, we focus here on processes of forest stand dynamics and demography, rather than carbon-nutrient cycle interactions, for investigating the GFDY hypothesis.

The GFDY hypothesis may result from the evolution of species' life-history strategies along the resource conservation versus exploitation spectrum, leading to fast-growing and short-lived species at one end, versus slow-growing and long-lived species at the other end. The GFDY trade-off could also be the outcome of demographic processes leading to a reduction of carbon residence time when tree growth is enhanced over time within individuals in a stand. While much empirical support for the GFDY hypothesis is based on variations across species (Brienen et al., 2015; Loehle, 1988; Wright et al., 2010), the emergent negative feedback between growth and biomass has also been argued to govern the response of forest stands to environmental changes in the absence of species replacement (Brienen et al., 2020; Bugmann & Bigler, 2011). Growth-longevity trade-offs within species have been found previously (Bigler & Veblen, 2009; Büntgen et al., 2019). The mechanisms underlying the negative feedback at the forest stand scale relate to competition for light and the tree's *C* balance. Accelerated tree growth and crown expansion under a constant canopy space constraint (Zeide, 1993) can drive the exclusion of short trees from the canopy, intensifying competition for light, and potentially enhancing their (density-driven) mortality. Faster tree growth can also lead to earlier attainment of a critical tree size where hydraulic, mechanical, or *C* balance constraints with increasing respiratory costs pose limits to further growth and may trigger mortality (Collalti et al., 2020; McDowell et al., 2022).

Allometric relationships of tree diameter, height, and crown area, combined with the canopy space constraint and its implication for density-driven mortality, lead to an emergent relationship between the mean tree size and the number of trees per unit area in closed-canopy forests. For monospecific and even-aged stands, this relationship has been described by a power-law relationship of the stand density and tree size in a closed forest stand, with the latter described by different variables, including biomass—Yoda's Law (Yoda et al., 1963) and mean stem diameter (Reineke, 1933). Forest data following Yoda's Law align along the so-called self-thinning line (STL)—the

linear relationship between tree number and mean tree size in a double-logarithmic plot. The use of STLs has a long tradition in forest management (Enquist et al., 1998; West et al., 1997) and research (Charru et al., 2012; Pretzsch, 2006). The position of the STL is often interpreted as a reflection of site quality (climate and soil properties) and is affected by species identity (Forrester et al., 2021a). Prescribed, site-specific, and temporally stationary STLs have been used in forest demography models (Mäkelä et al., 2000) for simulating forest stand dynamics and density-driven mortality (Landsberg & Waring, 1997).

A stationary STL implies that accelerated growth of trees will lead to their accelerated progression along the constant STL—consistent with the GFDY hypothesis. Hence, the relative change in biomass stocks should be small or even vanish, irrespective of the relative enhancement of growth, because variations in total stand-level biomass are small or even zero along the STL. Zero biomass variation along the STL follows if its slope is -1 (Mrad et al., 2020). Prior research has found no temporal change in the STL of unmanaged experimental forest plots in Europe over the past century (Pretzsch et al., 2014), or an upward shift of the STL in a CO_2 fertilization experiment (Kubiske et al., 2019). Thus, expanding the empirical basis for potential STL changes in unmanaged forests is needed and provides an approach to test the GFDY hypothesis.

To follow this approach, data from forest inventories are particularly valuable. However, forests are subject to continuous environmental change and forest inventory plots are often affected by prior management. Therefore, they cannot be assumed to have reached maturity and, consequently, a dynamic equilibrium of biomass stocks. Focusing on STLs for the analysis of trends in forest dynamics has the advantage that natural stand age-related changes in biomass and stand density can be controlled. Analyzing STL changes in long-term observations from unmanaged closed-canopy forest plots thus provides insights into persistent changes in forest stand dynamics and structure and offers an opportunity to investigate growth-longevity trade-offs driven by self-thinning and environmental changes.

Dynamic Global Vegetation Models (DGVMs) have been widely used for simulating the response of the terrestrial *C* cycle to global environmental change (Arora et al., 2019; Friedlingstein et al., 2022). They benefit from a detailed representation of the response of photosynthesis to a changing environment but have traditionally relied on simplifications of forest stand dynamics by resolving only an average individual tree (Fisher et al., 2019; Sitch et al., 2003), thus not accounting for size-dependent light competition and mortality (Bugmann et al., 2019; Evans, 2012; McDowell et al., 2011; Purves et al., 2008). Therefore, such models may lead to unrealistic simulations of growth-biomass relationships under environmental change (Friend et al., 2014; Pugh et al., 2020; Yu et al., 2019) and are not suitable to investigate mechanisms underlying the GFDY hypothesis (Needham et al., 2020). For example, a constant background mortality rate specified in models (Bugmann et al., 2019) may imply an overestimation of the changes in biomass stocks driven by changes in growth (*constant turnover rate*, Box 1), or a constant prescribed STL (Landsberg & Waring, 1997) may imply an underestimation of the same (*constant self-thinning*, Box 1).

Box 1. Approach to link changes in tree growth, biomass, and stand density

Mechanistic models (e.g., DGVMs) represent the carbon cycle in terrestrial ecosystems as a cascade of pools and fluxes (Randerson et al., 1997; Smith et al., 2013). The assumption that pool-specific residence times are independent of input fluxes and pool sizes, combined with constant relative allocation of fluxes to downstream pools and respiration, leads to linear systems dynamics (Luo & Weng, 2011; Weng et al., 2019; Xia et al., 2013), characterized by a proportional scaling of all fluxes and pools with the ultimate *C* input flux to the system—CO_2 assimilation by photosynthesis. Density-driven mortality is a process that introduces a negative relationship between the biomass *C* residence time and biomass production, thus triggering a feedback that leads to a deviation from linear systems dynamics. The analysis presented here is designed to diagnose this deviation from model outputs by investigating the relative change in biomass stocks (B) per unit relative change in tree growth (G), taken from simulations in this study as total ecosystem-level biomass production.

Three cases can be distinguished regarding the relative change in B per unit relative change in G, that is, $\frac{dB}{B}$ $vs.$ $\frac{dG}{G}$, which have different implications for changes in the self-thinning relationship (Figure 1).

(i) *Constant turnover rate* $\left(\frac{dB}{B} = \frac{dG}{G}\right)$. A relative enhancement of G leads to an equal relative enhancement of B and an upward shift of the STL. Steady-state B scales linearly with G (see Text S1 in Supporting Information S1). A linear response follows when the carbon residence time in biomass is not an explicit function of G or of B and constant relative to allocation.

(ii) *Accelerated turnover* $\left(\frac{dB}{B} < \frac{dG}{G}\right)$. This is an intermediate case that leads to a non-linear response where the relative increase in B is smaller than the relative increase in G. The residence time of biomass is reduced but an upward shift in the STL is still observed.

(iii) *Constant self-thinning* $\left(\frac{dB}{B} = 0\right.$ in the case of constant B along the STL). This case implies that a G enhancement accelerates trees' life cycles to a degree that nullifies a change in B, as implied in the GFDY hypothesis. Trees progress faster along a temporally invariant STL.

Considering the link between biomass and the STL, cases *i* and *ii* are marked with an upward shift of the STL, whereby the upward shift is larger for *i* than for *ii*. Investigating STL changes over time and in relation to variations in G thus yields insight into the (essentially unobservable but key) steady-state *G-B* relationship.

Here, we evaluated empirical and theoretical support for the GFDY hypothesis. We used long-term forest data from unmanaged stands in Switzerland to evaluate whether the STL has shifted through time and whether variations in the STL are influenced by stand-level growth. To investigate growth-STL changes, we first quantified growth trends across unmanaged forests in Switzerland. Then, using a vegetation demography model (BiomeE, Weng et al., 2015, 2019) that combines tree-level physiology and C balance with the simulation of competition for light and mortality, we explored the underlying mechanisms and investigated under which conditions persistent biomass stock increases result from growth enhancements.

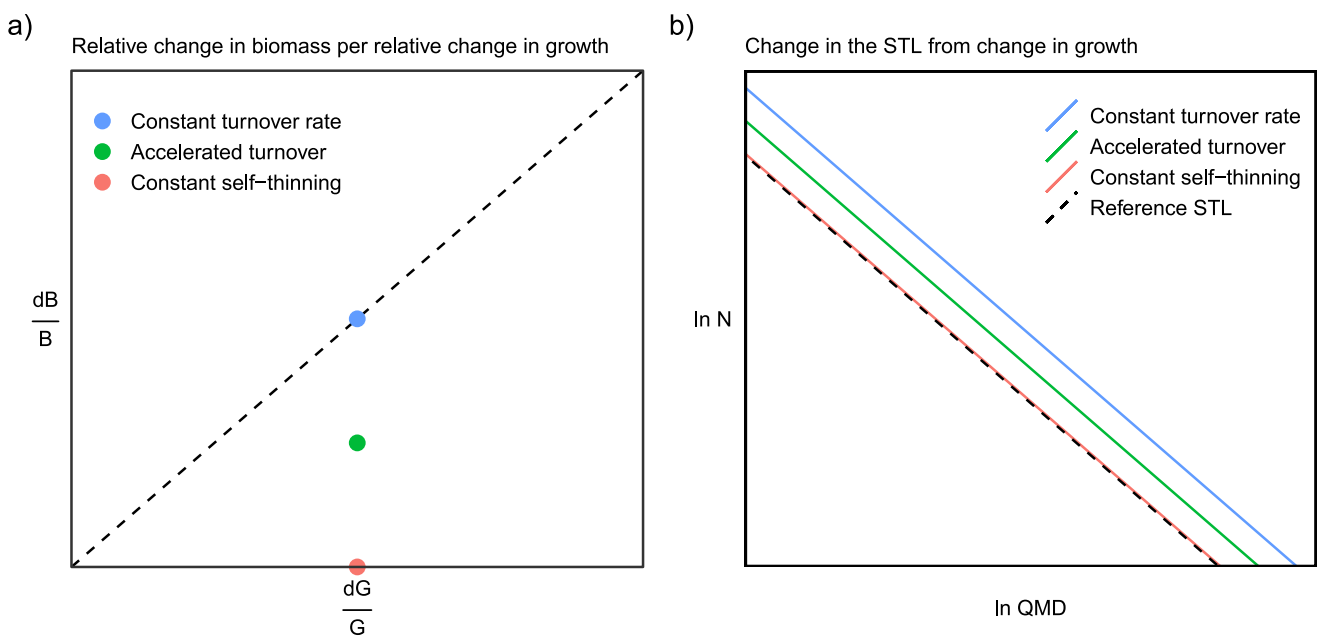

Figure 1. Conceptual model of biomass and STL responses to tree growth enhancement. (a) Responses of biomass stocks where an enhancement in growth may lead to no biomass increment (*constant self-thinning*, red circle) or to equal relative biomass increment (*constant turnover rate*, blue circle in the dashed 1:1 line). (b) Responses of the STL where growth enhancement may lead to no changes in the STL (*constant self-thinning*, red line on top of the lower solid black line, considered as a reference STL) or to a shift upwards in the STL (*constant turnover rate*, blue line). The intermediate stages of these two extreme assumptions representing an *accelerated turnover* are shown by a green circle (A) and line (B).

2. Material and Methods

2.1. Observed Forest Dynamics

2.1.1. Forest Data

Inventory data from mixed forests were obtained by combining observations from three sources: the Swiss National Forest Inventory (NFI) (Fischer & Traub, 2019), the Experimental Forest Management (EFM) network (Forrester et al., 2021b), and the Swiss Natural Forest Reserves (NFR) (Hobi et al., 2020). The data cover a range of latitudes between 46.0° and 47.8°, longitudes between 6.12° and 10.5°, and elevations between 334 and 2,154 m a.s.l. Mean temperature ranges from 0.6 to 12.0°C and annual precipitation exhibits a range of 736–2,391 mm per year (Brunner et al., 2019). The plots have an average size of 0.05 ha (NFI), 0.30 ha (EFM), and 0.40 ha (NFR). The measurement intervals in the data sets varied from 9 to 12 years, depending on the sampling design, growth rates, and environmental conditions (see Table S1 in Supporting Information S1 for more details on data characteristics). Based on specific information about each original data set, we selected unmanaged plots for which data were available from at least three censuses. We subset NFI plots free of management for at least 70 years prior to the first census. This information was derived from standardized interviews with the forest services (Portier et al., 2021). We considered EFM plots with no intervention since monitoring started, that is, 55 years on average. None of the NFR plots has experienced any management since the establishment of the forest reserves, with an average of 85 years. The negative relationship between stand density and mean tree size for all unmanaged plots from the three sources can be seen in Figure S1 of the Supporting Information S1. We applied a further filter to retain only data from plots for which the stand density (N) was in the upper Xth percentile within 30 bins (ca. 3 cm width) of average plot-level tree sizes, measured by the quadratic mean diameter (QMD). This approach allowed us to minimize the effects of natural past disturbances for which information is not recorded in the inventories (Brunet-Navarro et al., 2016). We performed a sensitivity analysis to select the best cut-off criterion (55th, 75th, and 90th percentile of plots). To ensure that all the selected plots have reached the STL, we identified as outliers those plots that fall below the $Q_1 - 1.5$ IQR or above $Q_3 + 1.5$ IQR for both N and QMD, with Q_1 and Q_3 being the first and third quartiles, respectively, and IQR the interquartile range. We finally applied the 75th percentile cut-off criterion, featuring a total of 259 plots, used for all subsequent analyses (102 from the NFI, 21 from the EFM, and 136 from the NFR), covering the years 1933–2019.

2.1.2. Tree and Stand-Level Measurements

In most cases, tree diameter at 1.3 m height (DBH, cm) was measured on all trees with DBH ≥ 4 cm (NFR), 8 cm (EFM), or 12 cm (NFI). For each stand, QMD (cm), stand density (N, trees ha^{-1}), and total biomass (B, kg C m^{-2}) were calculated for each measurement year. Biomass was estimated for the EFM and NFR plots following the allometric equations described in Forrester et al. (2017), where biomass is predicted from DBH and stand basal area. Species-specific equations included wood density (g cm^{-3}), or specific leaf area (SLA, m^2 kg^{-1}) and were also obtained from Forrester et al. (2017). The NFI data set provided biomass estimates following the methodology described in Fischer and Traub (2019). For these plots, biomass is calculated from the estimated volume of the living trees based on species-specific wood densities. Net stand biomass change (ΔB) was estimated as kg m^{-2} yr^{-1} by dividing the biomass difference from successive pairs of measurements by the number of years between censuses. We also quantified the mean tree biomass (kg C) as the arithmetic mean of stem biomass, and mean tree biomass change (kg C yr^{-1}) as the mean annual biomass increment across trees in the stand. We estimated the dominant species in the stand as the one with the highest basal area (m^2 ha^{-1}). For each plot, we compiled the information about the last management before the first census as a categorical variable. We specified six levels: <25, 25–50, 50–75, 75–100, 100–125, and >125 years. To evaluate the changes in species composition over time, we calculated the Bray-Curtis dissimilarity index (Bray & Curtis, 1957) by stem number comparing the same plot between censuses. The Bray-Curtis dissimilarity index estimated for each plot over time featured mean values of 0.26 (Table S1 in Supporting Information S1).

2.1.3. Data Analysis

To estimate trends in forest biomass and growth, we employed Linear Mixed-Effects models (LMMs). We examined the changes over time in tree and stand-level variables, including the quadratic mean diameter, stand density, stand biomass, stand net biomass increment, mean tree biomass, and mean tree biomass increment by comparing values between censuses and across the observation plots. All LMMs included *calendar year* and *mean tree size*

(DBH) as fixed factors and either plot identity or plot identity, dominant species, and year since last management as random intercepts for tree- and stand-level attributes, respectively (Figure S2 in Supporting Information S1). To better understand the relationship between biomass and growth, we reported the relative changes in biomass (*dB/B*) per unit of relative change in growth (*dG/G*) from the Swiss forests data (Figure S3 in Supporting Information S1). The self-thinning relationships were determined by regressing the logarithms of stand density and QMD. We used LMMs to evaluate how the STL depends on (a) *calendar year* and (b) *growth anomalies*. To estimate growth anomalies, we first fitted the stand-level ΔB against QMD using a Generalized Additive Mixed Model (GAMM) to remove the size effect on biomass accumulation and extracted the residual values (Figure S4 in Supporting Information S1). Additionally, we tested the robustness of results estimating growth anomalies from tree-level growth as the residuals of fitting mean tree biomass change against QMD in a similar fashion as done with stand-level growth. The general structure of the LMMs used for the STL analyses can be summarized as:

$$\ln(\mathrm{N}) = \beta_0 + \beta_1 \ln(\mathrm{QMD}) + \beta_2 X + b + c + d + \varepsilon \quad (1)$$

where stand density (N) is the dependent variable, and the fixed factors are QMD and X, which represent either *calendar year* or *growth anomalies*, both as continuous variables. The parameters b, c, and d are the random intercepts with plot identity, dominant species, and years since the last management as grouping variables and ε is the residual error term, which is assumed to be normally distributed. We included no interaction effect between QMD and the predictors (*calendar year* and *growth anomalies*) since our analysis's primary target was whether the STL has shifted in its vertical position and not its slope. We carried out additional tests to investigate interactions between the fixed effects and the influence of forest plot sizes in both LMMs. For the latter, we included *plot size* as an exogenous variable that could affect tree density. Model comparison was based on the Akaike Information Criterion corrected for small sample sizes (AICc), which selects the LMMs with the lowest AICc as the most parsimonious models (Burnham & Anderson, 2002). Parameter estimation was made using restricted maximum likelihood (REML), which estimates the variance parameters independently from the fixed effects (Zuur et al., 2009). We performed model diagnostics for the LMMs to check for linearity and homoscedasticity of the residuals. The percentages of variance explained by the fixed and random effects of the best model were obtained according to Nakagawa and Schielzeth (2013).

All statistical analyses were performed using the R statistical software version 4.0.5 (R Core Team, 2021). We fitted the GAMM using the *gamm4* R package (Wood, 2017) and the LMMs using the *lme4* R package (Bates et al., 2015) and calculated *p-values* with the *lmerTest* R package (Kuznetsova et al., 2017). The Bray-Curtis dissimilarity index was calculated using the *vegan* R package (Oksanen et al., 2022).

2.2. Modeling Approach

2.2.1. Model Description

We used the BiomeE model, implemented within the *rsofun* modeling framework (Stocker et al., 2021). BiomeE is a cohort-based vegetation demography model combining leaf-level ecophysiology, individual-level competition for light and soil resources, forest structural dynamics, and biogeochemical processes (Weng et al., 2015). The model links a standard photosynthesis model (Farquhar et al., 1980; Leuning et al., 1995) with tree growth and allometry, and scales from the geometry of individual trees to canopy structure and competition for light using the Perfect Plasticity Approximation (PPA) (Purves et al., 2008). The PPA assumes that individual tree stems and crowns are organized to fill the canopy irrespective of a tree's lateral positioning and thus form discrete canopy layers, within which all plants receive the same incoming radiation. Exclusion from the canopy and shading is determined based on a tree's height in relation to the critical height of the canopy (H^*), which is defined as the height of the shortest canopy tree, whereby the crown areas of canopy trees sum up to unity (minus a constant gap fraction). BiomeE allows for an explicit representation of cohorts of equally sized individuals and for a treatment of a tree's C balance and mortality. The model thus simulates size-structured competition for light, demographic processes, and dynamics of a forest stand. It has been comprehensively documented and evaluated against data from Eastern US temperate forests (Weng et al., 2015) and temperate to boreal forests in North America (Weng et al., 2017). For the present study, we used the model version described by Weng et al. (2019) and re-calibrated the model for simulations representing conditions in Central European forests (see Section 2.2.3). Since we focus here on links between growth and biomass, and since nitrogen-limitation effects are mediated predominantly

through processes affecting biomass production (Vicca et al., 2012), and not directly biomass stocks, we disabled the nitrogen limitation effects in all simulations.

2.2.2. Mortality Formulation and Parameterization

To test the GFDY hypothesis, an assumption about the structural dependence of the mortality rate (m, units of yr^{-1}) was defined for canopy trees (tree height above H^*). A size-dependent mortality rate was specified for the upper canopy layer, assuming the yearly mortality rate of the upper-canopy trees to follow a power law relationship with the tree's diameter (Equation 2). In this formulation, d is the diameter in cm, p_c is the calibrated parameter for the tree size mortality (scaling coefficient), and r is the exponent that determines the increase of the mortality rate with d in the canopy.

$$m_c = p_c \cdot d^r \tag{2}$$

An understory mortality rate was applied to the model setup, with higher mortality rates for the smaller and younger understory cohorts (Equation 3). This equation was adapted from Weng et al. (2015), where d is the diameter in cm, p_u is the calibrated parameter, and a,b are shape parameters for the understory mortality rate.

$$m_U = p_U \cdot \frac{1 + a \cdot e^{b \cdot d}}{1 + e^{b \cdot d}} \tag{3}$$

To evaluate the influence of the shape of the mortality rate parameterization applied to canopy trees (Equation 2), we investigated $r = 1.5$, 2.5, and 4.0 to implement a low, medium and high curvature of the tree diameter-mortality relationship. Parameters p_c and p_u were calibrated as described in Text S2 of the Supporting Information S1.

2.2.3. Simulations

All simulations were initiated with 0.05 saplings per m^2, an initial seedling size of 0.05 kg C per individual, and initial soil C and N pools. Model runs were done with a single species representing a generic temperate deciduous tree, chosen since the forest stand at the Lägeren site is dominated by *Fagus sylvatica*. Simulations were run for 1,500 years including a spin-up of 700 simulation years under constant environmental conditions to generate a steady-state as a dynamic equilibrium of all pools and fluxes. We used temporally constant model forcing data based on meteorological and CO_2 information obtained from site-level observations. Forcing variables include air and soil temperature (°C), precipitation (mm), radiation (W m^{-2}), atmospheric pressure (kPa), CO_2 (μmol mol^{-1}), wind speed (m s^{-1}), relative humidity (%), and soil water content (%).

To simulate tree growth enhancement, we applied a step-increase in the net photosynthesis after the model spin-up such that the light use efficiency of photosynthesis was elevated (eLUE) by two levels (+15% and +30%). Higher LUE and a resulting tree-level growth enhancement mimic the relief of limitations to carbon assimilation in a generic sense—be it via a growing season extension, enhanced nutrient inputs, relieving reductions of photosynthesis by low temperature, or increasing atmospheric CO_2. For each mortality parameterization ($r_{S1\text{-}S3}$), we ran the simulations for control and the two levels of eLUE (+15% and +30%).

We evaluated temporal changes in stand-level total biomass (B, kg C m^{-2}), annual total ecosystem-level biomass C production, in the context of model simulations referred to as *growth* (G, kg C m^{-2} yr^{-1}), and the C mass flux from tree mortality and tissue turnover, in the context of model simulations referred to as *mortality* (M, kg C m^{-2} yr^{-1}). Note that here, G and M are defined as mass fluxes of C, thus differing from tree-level growth, commonly expressed as an increment of diameter per unit of time or mortality defined as a fraction of dying trees per unit of time. We then calculated the relative changes in total stand-level biomass (dB/B), mortality (dM/M), carbon turnover rate (dk/k), and tree longevity (dL/L) by comparing averaged values over the last 600 years before and after the step increase in LUE and evaluated their ratio with respect to relative changes in growth (dG/G). The carbon turnover rate k (yr^{-1}) was defined as the ratio between M and B, that is, the inverse of the carbon residence time τ (yr; $k = 1/\tau$). Tree longevity was defined here as the age of the oldest tree cohort present in the ecosystem.

We also quantified the changes in the self-thinning trajectories resulting from eLUE conditions. We selected the last 600 years of the simulations to ensure that the steady-state had been reached. We tested if the STLs were influenced by the levels of LUE by fitting linear models (LMs) with stand density (log-scale) as the dependent variable, and QMD (log-scale) and LUE (as a proxy of growth enhancement) as predictors.

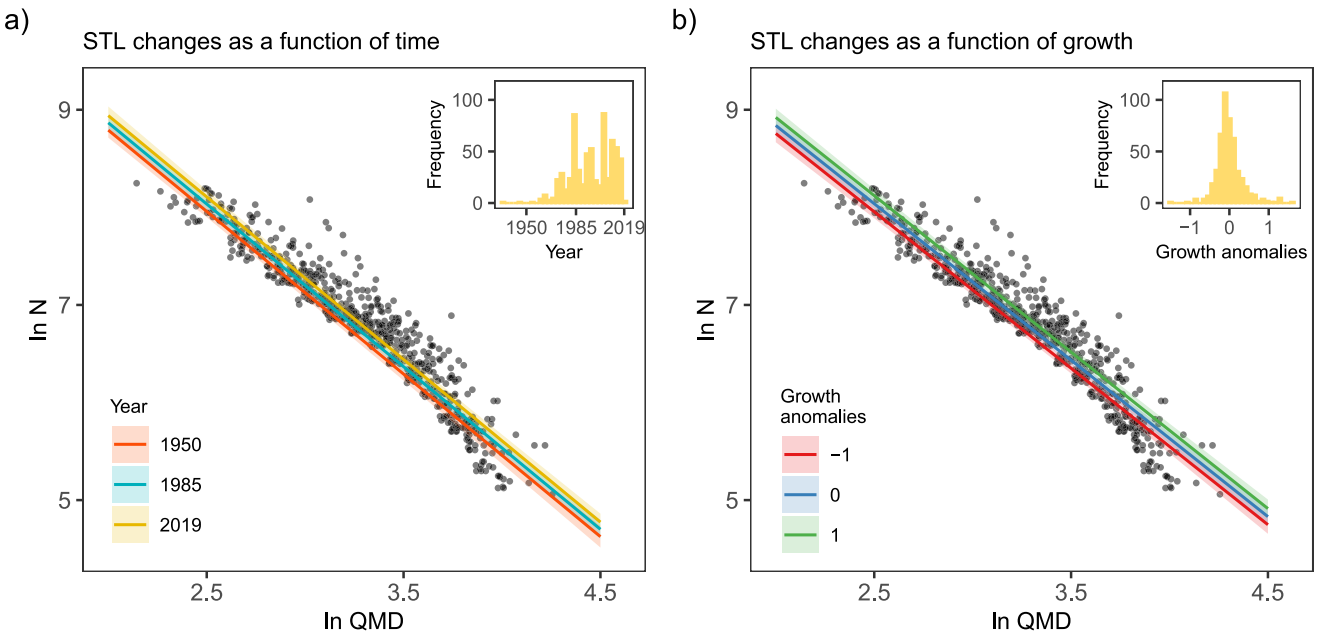

Figure 2. Stand density (N, trees ha^{-1}) as a function of QMD (cm) (both in log-scale) and (a) calendar year, or (b) growth anomalies over the study period for the subset of unmanaged plots (n = 267) of the pooled NFI (n = 108), EFM (n = 21), and NFR (n = 138) networks. Points represent data from plots selected within the 75th percentile and used for model fitting. Colored lines represent the fitted STLs and shaded areas represent the 95% confidence intervals. The embedded panels display the distributions of (a) calendar year and (b) growth anomalies for forest data used in the analyses.

3. Results

3.1. Observed Trends in Growth and Biomass

Across unmanaged forests in Switzerland, we found significant increases in the average stand-level tree sizes (QMD, 0.101 ± 0.008 cm yr^{-1}), stand biomass (0.215 ± 0.021 kg C m^{-2} yr^{-1}), and the mean tree biomass (6.403 ± 0.325 kg C yr^{-1}) over time, while stand density showed a significant decline (−6.944 ± 0.864 trees h a^{-1} yr^{-1}, Figure S2 and Table S2 in Supporting Information S1). These changes were accompanied by a significantly positive temporal trend in the mean tree biomass increment (0.053 ± 0.014 kg C yr^{-2}) and a non-significant positive trend in stand net biomass increment (0.688 ± 1.278 kg C m^{-2} yr^{-2}). Relative changes in the mean tree biomass increment were slightly greater than the relative change in biomass stocks (Figure S3 in Supporting Information S1).

3.2. Observational Changes in the Self-Thinning Relationships

The STL shifted upward over time, that is, for a given QMD, forest stands tend to have become denser through time (Figure 2a). Unmanaged Swiss forests exhibited a change in the STL as a function of growth anomalies, derived from stand-level ΔB, indicating also a spatial change across forest plots (Figure 2b). The LMMs identified a significant ($P < 0.001$) positive effect of both *calendar year* and *growth anomalies* on the intercept of the STL (see Table S3 in Supporting Information S1). This emerges from the patterns over time and across sites, thus indicating that the relationship between biomass and density has not been stationary but has shifted significantly over the past decades. Our findings were robust when analyzing the STL shifts dependent on tree growth anomalies (Table S4 in Supporting Information S1). The upward shift of the STL over time, that is, the average increase in density for a given QMD was 0.02%–0.04% per *year* when considering the 55th, 75th, and 90th percentiles of plots within average tree size bins. The average increase in density for a given QMD was 0.75%–1.26% per unit of growth anomaly (kg m^2 yr^{-1}) when considering the 55th, 75th, and 90th percentiles. The percentage of stand density variance explained by the fixed effects, that is, the marginal pseudo-R^2, was 85%–92% for both LMMs (Table S3 in Supporting Information S1).

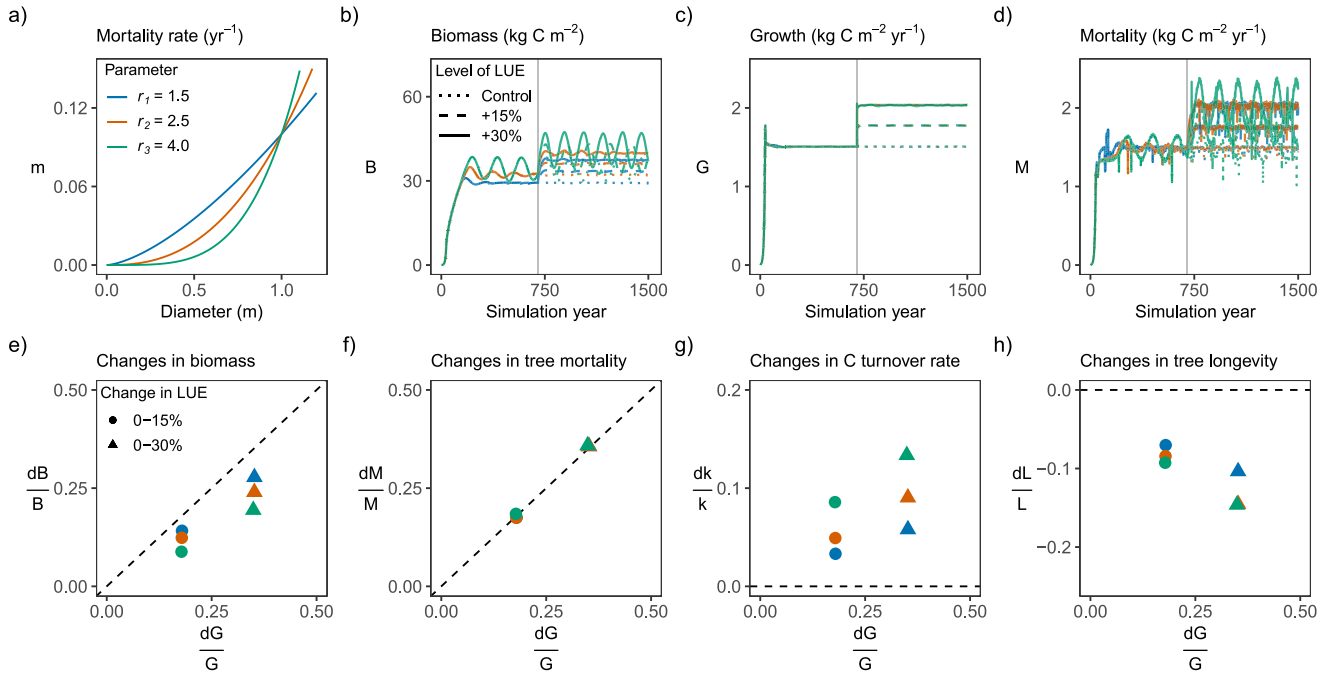

Figure 3. Model simulations for size-dependent mortality showing (a) different tree diameter-mortality shapes of canopy trees, (b) absolute changes in biomass, (c) growth, and (d) mortality over time, and (e) relative changes in biomass, (f) mortality, (g) carbon turnover rate and (h) longevity with respect to relative changes in growth. Colors show the mortality shape (low to high curvature), and line types/point shapes show simulated increases in LUE (15% and 30%). Vertical solid lines in panels (b–d) indicate the eLUE (year 700, after the model spin-up). The relative changes presented in panels (e–h) were calculated from the last 600 years of the simulations. Dashed lines following the 1:1 line (e) or the zero-value (g, h) represent the hypothetical *constant turnover rate* (case *i* described in Box 1).

The AICc selected the models with the main effects, that is, without interactions, as the most parsimonious models (Table S5 in Supporting Information S1). Similarly, the *plot size* predictor was not supported as a plausible determinant of tree density (Table S5 in Supporting Information S1) and was thus removed from the selected models. The residuals versus fitted (ln N) (Figures S5a and S5d in Supporting Information S1) did not indicate any deviations from a linear form and showed relatively constant variance across the fitted range. The residuals versus *ln QMD* (Figures S5b and S5e in Supporting Information S1), versus *year* (Figure S5c in Supporting Information S1), and versus *growth anomalies* (Figure S5f in Supporting Information S1) showed linearity in the independent variables.

3.3. Simulated Changes in Biomass Due To Growth Enhancement

In response to a 15% increase in LUE (or 30% eLUE, see values in brackets), *G* increased by 17% (or 35%), respectively, on average across the last 600 simulation years before and after the step increase (see *x*-axes in the bottom panels of Figure 3). The stronger relative stimulation of *G* compared to LUE is due to allocation to woody biomass in the model. *B* increased in response to *G* enhancements in all model setups (see step-increase after the spin-up), irrespective of the mortality parameterization (Figure 3b). However, the magnitude of the relative increase in *B* varied systematically with the shape of the mortality functions. Following a size-dependent mortality formulation, *B* increased by 9%–14% (or 19%–28%), and the higher the curvature of the mortality function, the lower the increase in *B*. Once a new steady-state of biomass stocks had been attained in the simulations, *M*, expressed in units of living biomass loss per unit area and time, attained the same average level as *G* in all model parameterizations (Figures 3c and 3d). This is a direct consequence of mass conservation but also indicates that under environmental changes and gradually increasing *G*, *M* increases in parallel, albeit with a lag. The considerable temporal variations of *B* and *M* reflect forest stand dynamics under dynamic equilibria before and after the step increase in eLUE and, consequently, growth. Simulations yield mean canopy mortality rates ranging between 0.040 and 0.057 yr^{-1}.

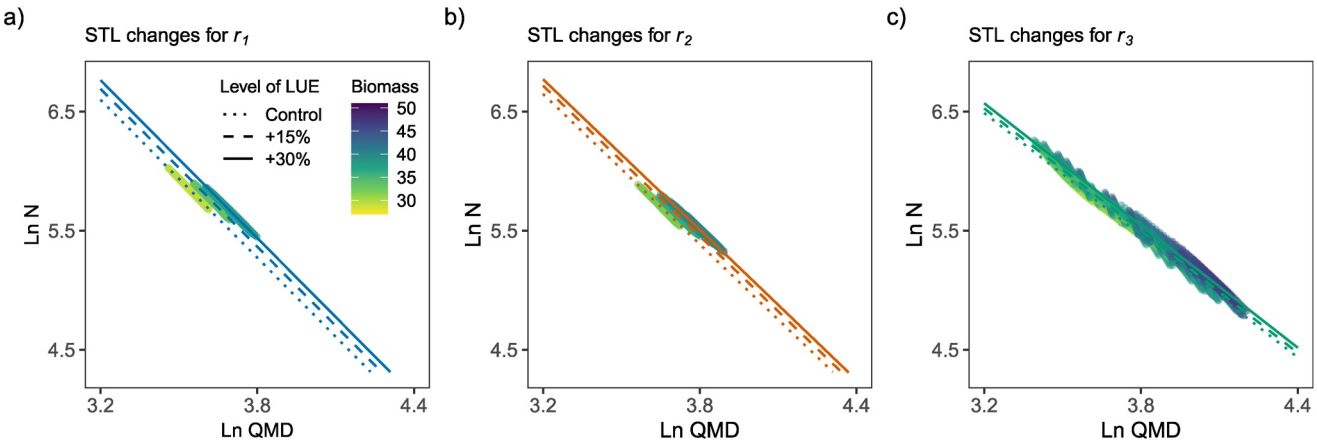

Figure 4. Simulated relationships between stand density (N, trees ha^{-1}) and quadratic mean diameter (QMD, m) for each mortality parameterization (r_1–r_3, line colors, a–c) under simulated increases in LUE (line types). The color of the points represents the total stand-level biomass (kg C m^{-2}).

Comparing the relative changes in biomass and carbon turnover time to the relative increase in growth yields insights into the (non-) linearity of the system (Box 1). Although *B* generally increased in response to increases in *G*—irrespective of mortality parameterization—the relative increase in *B* was always smaller than the relative increase in *G* (Figure 3e). The ratio of the respective relative changes varied substantially depending on the curvature of the mortality function. This indicates a distinct non-linearity in the system, introduced by the link between *G* and *B*, and illustrates that the degree of this non-linearity (deviation from the 1:1 line in Figure 3e) is governed by the curvature (non-linearity) of the mortality function. Reflecting mass balance constraints, relative increases in *G* and *M* are always identical, irrespective of the shape of the mortality function (Figure 3f).

Substantial variations in the relative increases in *B* for a given relative increase in *G* are reflected by the relative changes in the turnover rates and maximum tree longevity. Turnover rates increased (Figure 3g) and maximum tree longevity decreased (Figure 3h), irrespective of the curvature of the mortality function. Using a low curvature parameter of mortality ($r_1 = 1.5$ in Figure 3a), smaller relative changes in carbon turnover rates and tree longevity were simulated in response to growth enhancements than when using a pronounced curvature. Overall, relative increases in turnover rates were smaller than relative increases in *G*, thus leading to a positive response of *B* in all model setups.

A sensitivity analysis for the allometric scaling parameter (θ), relating diameter and biomass (Equation 2; Weng et al., 2019), confirmed the positive relationship between growth and biomass (Figure S6 in Supporting Information S1). For the plausible range of parameter values (Forrester et al., 2017), a non-linear *G*-*B* relationship was observed, with stronger relative increases in *B* simulated for higher values of θ.

We also tested whether model simulations capture the expected negative growth rate-longevity pattern found in the literature (Bigler & Veblen, 2009; Manusch et al., 2012). A strongly negative relationship between the mean tree growth rate and age of canopy trees was found (−0.99, −0.95), independently of the mortality parameterization (Figure S7 in Supporting Information S1). For all the simulations, enhanced growth rates led to shorter lifetimes of trees.

Taken together, the model simulates an acceleration of forest dynamics and a shortening of tree longevity when tree growth is enhanced and when simulating tree mortality as a size-dependent process. This is measured by the increase in turnover rates, which can be seen along with a reduction of the carbon residence time due to the speeding up of the life cycle (Figure S8a in Supporting Information S1). As trees grew faster, tree size distributions shifted toward larger sizes (Figure S8b in Supporting Information S1), despite the reduction in their longevity. This acceleration of forest dynamics did not preclude an increase in steady-state biomass stocks—irrespective of the assumptions regarding the mortality parameterization.

3.4. Simulated Changes in the Self-Thinning Relationships

Regardless of the mortality parameterization, eLUE simulations led to an upward shift in the simulated STL (Figure 4), suggesting a significant change in the maximum stand density (Table S6 in Supporting Information S1) and pointing to larger trees for a given stand density or denser stands for a given average tree size. Biomass was largely constant along the STLs and thus, an upward shift of the STL indicated that biomass increased at conditions where self-thinning is acting. Further, our results revealed the influence of the mortality parameterizations on the degree to which the STL is shifted in response to growth enhancements. Size-dependent mortality with a flatter shape (r_1) predicted a stronger increment of stand density for a given QMD (1.61% for 15% eLUE and 2.90% for 30% eLUE, Figure 4a), while functions with a higher curvature led to a weaker change in the STL (1.24% for 15% eLUE and 2.21% for 30% eLUE in the case of r_2, Figure 4b and 0.72% for 15% eLUE and 1.52% for 30% eLUE in the case of r_3, Figure 4c).

4. Discussion

We combined forest observations and model simulations to evaluate to what extent tree growth enhancements lead to persistent increases in forest biomass stocks. We found that the position of the STL has shifted upwards over time and as tree growth rates increased in unmanaged, closed-canopy forests in Switzerland. The observed trends were comparable to previously published estimates of stand net biomass increment (Brienen et al., 2015; Fang et al., 2014; Hubau et al., 2020; Walker et al., 2019). We demonstrated that growth enhancements are empirically associated and mechanistically linked to biomass stock changes and therefore relevant for understanding land *C* sink trends. Trends of biomass stocks in unmanaged Swiss forests estimated here (0.215 ± 0.021 kg C m^{-2} yr^{-1}) were of similar magnitude as biomass increases of European forests reported in Pan et al. (2011) (0.096 kg C m^{-2} yr^{-1})—albeit higher, as to be expected since we excluded plots where management reduced *C* stocks. Nevertheless, these numbers are on a magnitude that, when scaled across forest areas globally, add up to substantial contributions to global land *C* balance changes (Friedlingstein et al., 2022; Pan et al., 2011).

4.1. Accelerated Biomass Turnover Does Not Preclude Biomass Stock Increases

A positive net increment in biomass was simulated despite the reductions in carbon residence time and tree longevity. Simulations indicated a non-linear *G-B* relationship and an upward shift of the STL, as described by the *accelerated turnover* response (Box 1). These findings suggest that increasing biomass stocks and decreasing *C* residence times are not mutually exclusive. This reconciles reports of tree longevity reductions (Brienen et al., 2020; Bugmann & Bigler, 2011; Büntgen et al., 2019) with model predictions of increased forest biomass (Pugh et al., 2020; Terrer et al., 2019; Yu et al., 2019), both of which are consistent with the mechanistic understanding outlined here. None of the tree size-dependent mortality parametrizations implemented in the model suggested a *constant turnover rate* response (Box 1), as reported by models that account for a constant background mortality (Bugmann et al., 2019). None of the mortality assumptions, nor the data suggested a *constant self-thinning* response (Box 1), as underlined in the GFDY hypothesis. Yet, the ratio of relative changes in growth and biomass was critically affected by the shape of the mortality function. As we show here, the stronger the curvature in the size-mortality parameterization, the smaller the increase in biomass and the smaller the upward shift in the STL.

Substantial uncertainty is introduced by structural choices of tree mortality representations in vegetation models (Bugmann et al., 2019), and different parameterizations lead to contrasting results. For example, contrasting results by Brienen et al. (2020) indicated a lack of long-term biomass increments in response to a temporal trend toward increased growth. This is possibly related to their choice of a highly non-linear size-mortality parameterization, fitted to data that reflect a growth-longevity relationship across species—not a temporal relationship that underlies the forest inventory data analyzed here. Expanding the empirical basis for the relationship between relative changes in biomass stocks and productivity from diverse observations and experiments will be useful to better constrain models. We performed an additional quantitative comparison of the growth-biomass relationship from diverse estimates of their respective response to eCO_2 using data compiled by Walker et al. (2021). The

patterns in response to eCO_2-driven growth changes generally agree with the patterns seen in the Swiss forest data and our simulations: *dB/B* is generally smaller than *dG/G*, but not zero (Figure S9 in Supporting Information S1).

4.2. Growth-Biomass Links Affect the Land Carbon Cycle Response to Environmental Change

Carbon assimilation rates in terrestrial ecosystems have increased steadily as atmospheric CO_2 concentrations have risen over the past century (Campbell et al., 2017; Walker et al., 2021). In parallel, rising temperatures have led to an expansion of the growing season in winter-cold climates (Piao et al., 2019). Simultaneously, a substantial terrestrial *C* sink has persisted (Friedlingstein et al., 2022; Keeling et al., 1996). Yet, gains in carbon storage, driven by increased photosynthesis and growth, have been argued to be transitory (Brienen et al., 2020; Bugmann & Bigler, 2011; Büntgen et al., 2019; Körner, 2017), and ultimately limited by other resources (e.g., nutrients) and negative feedbacks arising through forest dynamics. The mechanisms linking changes in terrestrial photosynthesis and *C* storage remain uncertain (Andresen et al., 2016; Bugmann & Seidl, 2022; Davies-Barnard et al., 2020; Huntzinger et al., 2017) and a challenge for vegetation modeling because a multitude of processes and feedbacks are involved at different scales, ranging from leaves to trees, forest stands, ecosystems, the landscape, and the globe (Maschler et al., 2022; Walker et al., 2021). The *G-B* relationships and the STL shifts described here are relevant for the propagation of effects by increased growth to the carbon balance at the scale of a forest stand. Our focus on the ratio of relative changes in *G* and *B* sheds light on processes that link the two quantities, independent of their absolute magnitudes, and avoids the influence of processes that act directly on biomass productivity and its relation to photosynthesis—for example, through effects of soil nutrient scarcity (Vicca et al., 2012). However, simultaneous biomass productivity enhancements and shifts in relative allocation toward short-lived fine root biomass, as often seen under eCO_2 (Drake et al., 2011; Song et al., 2019; Terrer et al., 2018), modify *G-B* relationships and should be considered in future studies.

With the advent of demography representations in global vegetation and terrestrial carbon cycle models, there is a need for constraining alternative process representations with observations. Novel cohort-based vegetation demography models (Fisher et al., 2018), such as the BiomeE, resolve tree age and height structure and enable a more mechanistic treatment of forest dynamics and tree mortality. This yields a foundation for project responses to environmental change and enables globally distributed forest inventory data to be used for constraining the models. However, observations are sparse due to the long timescale of forest demographic processes. The approach taken in this study enabled us to test the GFDY hypothesis via the STL changes observable from data that inform the unobservable (simulated) steady-state biomass response to growth enhancement.

4.3. An Emergent, Not Causal, Negative Growth Rate-Longevity Relationship

In our simulations, a growth enhancement skews the distribution of trees to larger sizes, decreases the number of trees in the canopy, and increases tree numbers in the understory. Under conditions of higher growth, this replacement is accelerated, leading to higher mortality rates, lower tree longevity, and a subsequent decrease in carbon residence time (Needham et al., 2020). This negative growth-longevity relationship is an emergent behavior of forest stand dynamics in response to the environment and parallels a similar relationship across species reflecting life-history strategies and trade-offs (Brienen et al., 2015). However, these patterns are not underlined by a direct causal and negative relationship between growth and longevity within individual plants. In contrast, within-stand and within-species variations indicate that fast-growing trees have lower, not higher, mortality probabilities (Cailleret et al., 2019; Hülsmann et al., 2018), and tree mortality is often preceded by growth reductions—not increases (Bigler & Bugmann, 2004; Cailleret et al., 2016). Hence, the emergent negative growth rate-tree longevity relationships across time and across forest plots should not serve as a basis for mortality parameterizations in models.

4.4. Endogenous and Exogenous Factors Affecting Carbon Residence Times

It is important to distinguish between changes in carbon residence times caused by endogenous (i.e., tree growth, density-driven mortality) and exogenous factors (e.g., climate, climate-driven disturbances). Here, we focused on the former. Observations from tropical forests have suggested that increases in productivity combined with persistently higher mortality led to shorter carbon residence times (Brienen et al., 2015; Hubau et al., 2020).

Still, no clear consensus exists about the trade-offs between growth and tree longevity and their temporal changes within species (Cailleret et al., 2017). Changes in tree mortality (DeSoto et al., 2020) and size-dependent survival (Johnson et al., 2018) have been linked to changes in climate and the environment. Disturbances are becoming more frequent (Sommerfeld et al., 2018), leading to enhanced tree mortality around the world (Senf et al., 2018). A recent study also pointed to the contribution of large trees to changes in aboveground biomass and carbon turnover rate across forests (Needham et al., 2022), which could be especially relevant under changes in disturbance regimes.

Evidence suggests that carbon residence times in forest biomass have declined in the past (Yu et al., 2019) and may be reduced by future climate change. Rising temperature, vapor pressure deficit (VPD) levels, and more frequent drought episodes can reduce photosynthetic C uptake as trees close their stomata to prevent hydraulic failure (McDowell et al., 2020; Schwalm et al., 2017). This may cancel any potential benefit from elevated atmospheric CO_2, leading to lower growth (Yuan et al., 2019) and higher mortality (Bauman et al., 2022). Climate-driven risks may thus lead to higher competition for water and override growth-related forest density trends (Anderegg et al., 2020). Our findings highlight that growth enhancement causes simultaneous increases in biomass and decreases in carbon residence times and tree lifespans and is to be understood as representing effects within species in the absence of exogenous factors (i.e., disturbance) that may reduce tree lifetimes in a future climate.

4.5. Interpreting Self-Thinning Relationships

The simulated growth-biomass relationship is qualitatively consistent with the empirical results suggesting temporal and spatial trends in the STL, with a link to growth variations across plots and time. We applied the STL concept to mixed, often uneven-aged forests in Switzerland to detect whether constraints governed by density-driven mortality have been relieved. Traditionally, the focus of the STL has been restricted to even-aged monospecific stands, and the power-law exponent (i.e., the slope of the STL) was proposed to be constant and universal (Reineke, 1933; Westoby, 1984; Yoda et al., 1963). Further studies showed that the STL directly reflects allometric and metabolic scaling, linking tree size, stand structure, and biomass stocks (Enquist et al., 2009). Generally, higher intercepts and slopes are associated with fertile soils (Bi, 2004; Morris & Charles Morris, 2003), which can reach higher tree densities (Charru et al., 2012; Weiskittel et al., 2008).

Self-thinning dynamics have also been described in mixed forests (Midgley, 2001; Mrad et al., 2020) and the application has been generalized to multispecific stands (Forrester et al., 2021a; Rivoire & Le Moguedec, 2012). The self-thinning relationship emerges from density-driven mortality due to resource competition between individuals, neglecting mortality due to external factors. Our approach excluded areas under management, and we selected plots featuring high density for a given QMD as those subject to self-thinning. By doing so, we ensured to remove or at least minimize external effects from natural or anthropogenic past disturbances. Indeed, we found a negative and largely linear relationship between the number and size of trees in a forest stand, like those seen in monospecific, even-aged stands.

The STL approach allowed us to control for stand age effects on biomass, thus revealing shifts in biomass storage without relying on observations of mature stands. Our empirical analyses suggested a tendency toward denser stands for a given QMD over time and indicated that stand density is related to growth vigor. These results are consistent with empirical evidence from Kubiske et al. (2019) who reported increasing intercepts of the STLs under higher CO_2, leading to stand biomass increases in the long term. Recent findings also indicate that climatic variables (Brunet-Navarro et al., 2016; Forrester et al., 2021a) influence the STL, although other studies found that it remained constant over time (Pretzsch et al., 2014). Importantly, the STL in mixed forests can also change when the relative proportion of species changes (Reyes-Hernandez et al., 2013), for example, due to succession. However, the Swiss forest stands used in our analyses did not feature strong shifts in species composition across plots (see Table S1 in Supporting Information S1). Our analysis also considered species effects by including the dominant species per plot as a random factor to control for species composition.

Further, our framework of evaluating changes in the STL in observations and simulations (with one PFT) avoids confounding effects to the largest extent possible. Our findings confirm that STLs are not static, simply reflecting edaphic factors, but are changing over time and as growth rate increases. This is relevant for forest management, which often relies on the STL to inform wood harvesting and plantation management (Nagel et al., 2017). Earlier research has indicated that the slope of the STL may change as forest stands mature (Duncanson et al., 2015).

However, we did not find a clear pattern in the residuals of fitted STL with average tree size (Figure S5 in Supporting Information S1), and the relationships of STL positions with time and growth are robust against excluding data from the stands with particularly low or high average tree sizes (Figure S10 and Table S7 in Supporting Information S1). Assuming a stationary self-thinning trajectory and a steeper slope as stands mature, would imply a downward shift of the fitted STL. Future work should investigate if shifts in these relationships also occur in primary forests along broader environmental gradients.

4.6. Robustness of Results and Open Challenges

Our study shows that the ratio of relative changes in growth and biomass is subject to the representation of mortality in the model. We tested the sensitivity to size-dependent mortality parameterization choices (Figure 3a). However, other processes affecting resource accessibility to tree individuals and their neighbors may influence the *G-B* relationship. This includes parameters regarding allometric scaling, height-dependent crown organization, and light penetration in the canopy. We additionally evaluated the influence of alternative allometric scaling parameters (Figure S6 in Supporting Information S1). This indicated that the finding of generally positive biomass changes in response to growth increases is robust against a wider choice of model formulations. In BiomeE, the PPA warrants that the tree crowns fill gaps in the canopy through phototropism (Purves et al., 2007, 2008). The PPA gives a competitive advantage to taller trees that reach the top canopy and access full sunlight. However, this ignores gap-phase dynamics where small trees can, for a short time, access full sunlight when an adjacent tree dies. Weng et al. (2015) also tested the BiomeE model by randomly choosing small seedlings to fill the canopy gaps, which did not change the overall model behavior.

Tree mortality is often caused by multiple interacting drivers, and it is often difficult to identify long-term trends (McMahon et al., 2019). Understanding the causes of observed mortality trends will help to improve the way mortality is treated in vegetation demography models, which is critical for accurate projections of global terrestrial carbon storage (Friend et al., 2014). Future work including model intercomparisons to test simulations with a set of alternative models would help inform the generality of the positive *G-B* relationship found here. Importantly, to evaluate model reliability in accurately simulating *G-B* links, a focus may be set on whether they capture self-thinning relationships (slope, position, and their change over time) as suggested by the data. Thus, combined analyses of models and forest observations will be needed to project how changes in environmental conditions will affect competition for resources and forest dynamics in a future climate (McDowell et al., 2018). Still, experimental insights are lacking for how mortality is influenced by CO_2 fertilization of photosynthesis and growth (Walker et al., 2021)—a key question to understand and project long-term changes in biomass. Many long-term monitoring plots are required to better understand the links between growth and biomass and to constrain influential, yet not directly observable model parameters (Needham et al., 2018).

5. Conclusions

Forest responses to global environmental changes are still unclear and difficult to study due to multiple interactions and anthropogenic disturbances. We focus on the mechanisms of forest stand dynamics and demography that determine the link between changes in tree growth and stand-level biomass stocks. We find that unmanaged closed-canopy forests in Switzerland have become denser for a given average tree size over the past six decades, and we identify a positive relationship between tree growth and stand density. These observations are consistent with simulations of a vegetation demography model showing that growth enhancements lead to increases in forest biomass and changes in the self-thinning relationship. However, simulated relative changes in biomass are smaller than relative changes in growth, indicating an apparent reduction in carbon residence time. We show that this effect critically depends on the mortality parameterizations. This data-supported mortality modeling yields new insights into the causes of the currently observed terrestrial carbon sinks. Thus, our study provides a better understanding of whether and how growth enhancements drive higher *C* storage in biomass—a key open question in carbon cycle research and highly relevant in the context of climate and Earth system changes.

Conflict of Interest

The authors declare no conflicts of interest relevant to this study.

Data Availability Statement

Data analyses and evaluations were based on data from the following Swiss Forest Monitoring networks: (a) the Swiss National Forest Inventory (NFI, https://www.lfi.ch), (b) the Experimental Forest Management (EFM, https://www.envidat.ch/dataset/the-experimental-forest-management-network), and (c) the Natural Forest Reserves (NFR, https://www.envidat.ch/dataset/forest-reserves-monitoring-in-switzerland). Model calibration was based on data from the Swiss Long-term Forest Ecosystem Research (LWF, https://www.envidat.ch/organization/about/lwf). Data are available under request to the specific networks. Code for the data analyses and model simulations of this study is available at the GitHub repository geco-bern/GFDY, https://doi.org/10.5281/zenodo.7326085.

Acknowledgments

We gratefully acknowledge the data providers and their long-term work to maintain and measure the different forest plots network. LM and BDS were funded by the Swiss National Science Foundation Grant PCEFP2_181115. We acknowledge WSL and ETH and their scientists, technicians, and data managers who designed, carried out and maintained the measurements on the permanent monitoring plots used in this study. The Swiss Forest Reserve Research Network is supported by the Swiss Federal Office for the Environment (FOEN), WSL, and ETH Zurich. This work is a contribution to the LEMONTREE (Land Ecosystem Models based On New Theory, obseRvations, and ExperimEnts) project, funded through the generosity of Eric and Wendy Schmidt by recommendation of the Schmidt Futures program. BDS acknowledges support from this project. EW acknowledges the support from the NASA Modeling, Analysis, and Prediction Program (award numbers: 80NSSC21K1496 and NNH10ZDA001N) for the development of the BiomeE model.

References

Ainsworth, E. A., & Long, S. P. (2005). What have we learned from 15 years of free-air CO_2 enrichment (FACE)? A meta-analytic review of the responses of photosynthesis, canopy properties and plant production to rising CO_2. *New Phytologist*, *165*(2), 351–371. https://doi.org/10.1111/j.1469-8137.2004.01224.x

Anderegg, W. R. L., Ballantyne, A. P., Smith, W. K., Majkut, J., Rabin, S., Beaulieu, C., et al. (2015). Tropical nighttime warming as a dominant driver of variability in the terrestrial carbon sink. *Proceedings of the National Academy of Sciences of the United States of America*, *112*(51), 15591–15596. https://doi.org/10.1073/pnas.1521479112

Anderegg, W. R. L., Trugman, A. T., Badgley, G., Anderson, C. M., Bartuska, A., Ciais, P., et al. (2020). Climate-driven risks to the climate mitigation potential of forests. *Science*, *368*(6497). https://doi.org/10.1126/science.aaz7005

Andresen, L. C., Müller, C., de Dato, G., Dukes, J. S., Emmett, B. A., Estiarte, M., et al. (2016). Shifting impacts of climate change. In *Advances in ecological research* (pp. 437–473). Elsevier. https://doi.org/10.1016/bs.aecr.2016.07.001

Arora, V. K., Katavouta, A., Williams, R. G., Jones, C. D., Brovkin, V., Friedlingstein, P., et al. (2019). Carbon-concentration and carbon-climate feedbacks in CMIP6 models, and their comparison to CMIP5 models. https://doi.org/10.5194/bg-17-4173-2020

Bates, D., Mächler, M., Bolker, B., & Walker, S. (2015). Fitting linear mixed-effects models using lme4. *Journal of Statistical Software*, *67*(1). https://doi.org/10.18637/jss.v067.i01

Bauman, D., Fortunel, C., Delhaye, G., Malhi, Y., Cernusak, L. A., Bentley, L. P., et al. (2022). Tropical tree mortality has increased with rising atmospheric water stress. *Nature*, *608*(7923), 528–533. https://doi.org/10.1038/s41586-022-04737-7

Bi, H. (2004). Stochastic Frontier analysis of a classic self-thinning experiment. *Austral Ecology*, *29*(4), 408–417. https://doi.org/10.1111/j.1442-9993.2004.01379.x

Bigler, C., & Bugmann, H. (2004). Predicting the time of tree death using dendrochronological data. *Ecological Applications*, *14*(3), 902–914. https://doi.org/10.1890/03-5011

Bigler, C., & Veblen, T. T. (2009). Increased early growth rates decrease longevities of conifers in subalpine forests. *Oikos*, *118*(8), 1130–1138. https://doi.org/10.1111/j.1600-0706.2009.17592.x

Bradford, J. B., Birdsey, R. A., Joyce, L. A., & Ryan, M. G. (2008). Tree age, disturbance history, and carbon stocks and fluxes in subalpine Rocky Mountain forests. *Global Change Biology*, *14*(12), 2882–2897. https://doi.org/10.1111/j.1365-2486.2008.01686.x

Bray, J. R., & Curtis, J. T. (1957). An ordination of the upland forest communities of southern Wisconsin. *Ecological Monographs*, *27*(4), 325–349. https://doi.org/10.2307/1942268

Brienen, R. J. W., Caldwell, L., Duchesne, L., Voelker, S., Barichivich, J., Baliva, M., et al. (2020). Forest carbon sink neutralized by pervasive growth-lifespan trade-offs. *Nature Communications*, *11*(1), 4241. https://doi.org/10.1038/s41467-020-17966-z

Brienen, R. J. W., Phillips, O. L., Feldpausch, T. R., Gloor, E., Baker, T. R., Lloyd, J., et al. (2015). Long-term decline of the Amazon carbon sink. *Nature*, *519*(7543), 344–348. https://doi.org/10.1038/nature14283

Brunet-Navarro, P., Sterck, F. J., Vayreda, J., Martinez-Vilalta, J., & Mohren, G. M. J. (2016). Self-thinning in four pine species: An evaluation of potential climate impacts. *Annals of Forest Science*, *73*(4), 1025–1034. https://doi.org/10.1007/s13595-016-0585-y

Brunner, M. I., Björnsen Gurung, A., Zappa, M., Zekollari, H., Farinotti, D., & Stähli, M. (2019). Present and future water scarcity in Switzerland: Potential for alleviation through reservoirs and lakes. *Science of the Total Environment*, *20*(666), 1033–1047. https://doi.org/10.1016/j.scitotenv.2019.02.169

Bugmann, H., & Bigler, C. (2011). Will the CO_2 fertilization effect in forests be offset by reduced tree longevity? *Oecologia*, *165*(2), 533–544. https://doi.org/10.1007/s00442-010-1837-4

Bugmann, H., & Seidl, R. (2022). The evolution, complexity and diversity of models of long-term forest dynamics. *Journal of Ecology*, *110*(10), 2288–2307. https://doi.org/10.1111/1365-2745.13989

Bugmann, H., Seidl, R., Hartig, F., Bohn, F., Brůna, J., Cailleret, M., et al. (2019). Tree mortality submodels drive simulated long-term forest dynamics: Assessing 15 models from the stand to global scale. *Ecosphere*, *10*(2), e02616. https://doi.org/10.1002/ecs2.2616

Büntgen, U., Krusic, P. J., Piermattei, A., Coomes, D. A., Esper, J., Myglan, V. S., et al. (2019). Limited capacity of tree growth to mitigate the global greenhouse effect under predicted warming. *Nature Communications*, *10*(1), 2171. https://doi.org/10.1038/s41467-019-10174-4

Burnham, K. P., & Anderson, D. R. (2002). *Model selection and multimodel inference: A practical information-theoretic approach*. Springer Science & Business Media. https://doi.org/10.1007/b97636

Cailleret, M., Bigler, C., Bugmann, H., Camarero, J. J., Cˇufar, K., Davi, H., et al. (2016). Towards a common methodology for developing logistic tree mortality models based on ring-width data. *Ecological Applications*, *26*(6), 1827–1841. https://doi.org/10.1890/15-1402.1

Cailleret, M., Dakos, V., Jansen, S., Robert, E. M. R., Aakala, T., Amoroso, M. M., et al. (2019). Early-warning signals of individual tree mortality based on annual radial growth. *Frontiers in Plant Science*, *9*. https://doi.org/10.3389/fpls.2018.01964

Cailleret, M., Jansen, S., Robert, E. M. R., Desoto, L., Aakala, T., Antos, J. A., et al. (2017). A synthesis of radial growth patterns preceding tree mortality. *Global Change Biology*, *23*(4), 1675–1690. https://doi.org/10.1111/gcb.13535

Campbell, J. E., Berry, J. A., Seibt, U., Smith, S. J., Montzka, S. A., Launois, T., et al. (2017). Large historical growth in global terrestrial gross primary production. *Nature*, *544*(7648), 84–87. https://doi.org/10.1038/nature22030

Charru, M., Seynave, I., Morneau, F., Rivoire, M., & Bontemps, J.-D. (2012). Significant differences and curvilinearity in the self-thinning relationships of 11 temperate tree species assessed from forest inventory data. *Annals of Forest Science*, *69*(2), 195–205. https://doi.org/10.1007/s13595-011-0149-0

Cole, C. T., Anderson, J. E., Lindroth, R. L., & Waller, D. M. (2009). Rising concentrations of atmospheric CO_2 have increased growth in natural stands of quaking aspen (*Populus tremuloides*). *Global Change Biology*, *16*(8), 2186–2197. https://doi.org/10.1111/j.1365-2486.2009.02103.x

Collalti, A., Tjoelker, M. G., Hoch, G., Mäkelä, A., Guidolotti, G., Heskel, M., et al. (2020). Plant respiration: Controlled by photosynthesis or biomass? *Global Change Biology*, *26*(3), 1739–1753. https://doi.org/10.1111/gcb.14857

Davies-Barnard, T., Meyerholt, J., Zaehle, S., Friedlingstein, P., Brovkin, V., Fan, Y., et al. (2020). Nitrogen cycling in CMIP6 land surface models: Progress and limitations. https://doi.org/10.5194/bg-17-5129-2020

DeSoto, L., Cailleret, M., Sterck, F., Jansen, S., Kramer, K., Robert, E. M. R., et al. (2020). Low growth resilience to drought is related to future mortality risk in trees. *Nature Communications*, *11*(1), 545. https://doi.org/10.1038/s41467-020-14300-5

Drake, J. E., Gallet-Budynek, A., Hofmockel, K. S., Bernhardt, E. S., Billings, S. A., Jackson, R. B., et al. (2011). Increases in the flux of carbon belowground stimulate nitrogen uptake and sustain the long-term enhancement of forest productivity under elevated CO_2. *Ecology Letters*, *14*(4), 349–357. https://doi.org/10.1111/j.1461-0248.2011.01593.x

Duncanson, L. I., Dubayah, R. O., & Enquist, B. J. (2015). Forest allometric variability in the United States. *Global Ecology and Biogeography*, *24*(12), 1465–1475. https://doi.org/10.1111/geb.12371

Ellsworth, D. S., Anderson, I. C., Crous, K. Y., Cooke, J., Drake, J. E., Gherlenda, A. N., et al. (2017). Elevated CO_2 does not increase eucalypt forest productivity on a low-phosphorus soil. *Nature Climate Change*, *7*(4), 279–282. https://doi.org/10.1038/nclimate3235

Enquist, B. J., Brown, J. H., & West, G. B. (1998). Allometric scaling of plant energetics and population density. *Nature*, *395*(6698), 163–165. https://doi.org/10.1038/25977

Enquist, B. J., West, G. B., & Brown, J. H. (2009). Extensions and evaluations of a general quantitative theory of forest structure and dynamics. *Proceedings of the National Academy of Sciences of the United States of America*, *106*(17), 7046–7051. https://doi.org/10.1073/pnas.0812303106

Evans, M. R. (2012). Modelling ecological systems in a changing world. *Philosophical Transactions of the Royal Society of London B Biological Sciences*, *367*(1586), 181–190. https://doi.org/10.1098/rstb.2011.0172

Fang, J., Kato, T., Guo, Z., Yang, Y., Hu, H., Shen, H., et al. (2014). Evidence for environmentally enhanced forest growth. *Proceedings of the National Academy of Sciences of the United States of America*, *111*(26), 9527–9532. https://doi.org/10.1073/pnas.1402333111

Farquhar, G. D., von Caemmerer, S., & Berry, J. A. (1980). A biochemical model of photosynthetic CO_2 assimilation in leaves of C 3 species. *Planta*, *149*(1), 78–90. https://doi.org/10.1007/bf00386231

Fatichi, S., Pappas, C., Zscheischler, J., & Leuzinger, S. (2019). Modelling carbon sources and sinks in terrestrial vegetation. *New Phytologist*, *221*(2), 652–668. https://doi.org/10.1111/nph.15451

Fischer, C. & Traub, B. (Eds.) (2019). Swiss National Forest Inventory—Methods and models of the fourth assessment, *Managing forest ecosystems* (Vol. 35, p. 431). Springer Nature. https://doi.org/10.1007/978-3-030-19293-8

Fisher, R. A., Koven, C. D., Anderegg, W. R. L., Christoffersen, B. O., Dietze, M. C., Farrior, C. E., et al. (2018). Vegetation demographics in Earth system models: A review of progress and priorities. *Global Change Biology*, *24*(1), 35–54. https://doi.org/10.1111/gcb.13910

Fisher, R. A., Wieder, W. R., Sanderson, B. M., Koven, C. D., Oleson, K. W., Xu, C., et al. (2019). Parametric controls on vegetation responses to biogeochemical forcing in the CLM5. *Journal of Advances in Modeling Earth Systems*, *11*(9), 2879–2895. https://doi.org/10.1029/2019ms001609

Fleischer, K., Rammig, A., De Kauwe, M. G., Walker, A. P., Domingues, T. F., Fuchslueger, L., et al. (2019). Amazon forest response to CO_2 fertilization dependent on plant phosphorus acquisition. *Nature Geoscience*, *12*(9), 736–741. https://doi.org/10.1038/s41561-019-0404-9

Forrester, D. I., Baker, T. G., Elms, S. R., Hobi, M. L., Ouyang, S., Wiedemann, J. C., et al. (2021a). Self-thinning tree mortality models that account for vertical stand structure, species mixing and climate. *Forest Ecology and Management*, *487*, 118936. https://doi.org/10.1016/j.foreco.2021.118936

Forrester, D. I., Schmid, H., & Nitzsche, J. (2021b). The experimental forest management network. *EnviDat*. https://doi.org/10.16904/envidat.213

Forrester, D. I., Tachauer, I. H. H., Annighoefer, P., Barbeito, I., Pretzsch, H., Ruiz-Peinado, R., et al. (2017). Generalized biomass and leaf area allometric equations for European tree species incorporating stand structure, tree age and climate. *Forest Ecology and Management*, *396*, 160–175. https://doi.org/10.1016/j.foreco.2017.04.011

Frelich, L. E. (2002). *Forest dynamics and disturbance regimes: Studies from temperate evergreen-deciduous forests*. Cambridge University Press. Cambridge.

Friedlingstein, P., Jones, M. W., O'Sullivan, M., Andrew, R. M., Bakker, D. C. E., Hauck, J., et al. (2022). Global carbon budget 2021.

Friend, A. D., Lucht, W., Rademacher, T. T., Keribin, R., Betts, R., Cadule, P., et al. (2014). Carbon residence time dominates uncertainty in terrestrial vegetation responses to future climate and atmospheric CO_2. *Proceedings of the National Academy of Sciences of the United States of America*, *111*(9), 3280–3285. https://doi.org/10.1073/pnas.1222477110

Gloor, M., Phillips, O. L., Lloyd, J. J., Lewis, S. L., Malhi, Y., Baker, T. R., et al. (2009). Does the disturbance hypothesis explain the biomass increase in basin-wide Amazon forest plot data? *Global Change Biology*, *15*(10), 2418–2430. https://doi.org/10.1111/j.1365-2486.2009.01891.x

Hobi, M., Stillhard, J., Projer, G., Mathys, A., Bugmann, H., & Brang, P. (2020). Forest reserves monitoring in Switzerland. *EnviDat*. https://doi.org/10.16904/envidat.141

Hovenden, M. J., Leuzinger, S., Newton, P. C. D., Fletcher, A., Fatichi, S., Lüscher, A., et al. (2019). Globally consistent influences of seasonal precipitation limit grassland biomass response to elevated CO_2. *Nature Plants*, *5*(2), 167–173. https://doi.org/10.1038/s41477-018-0356-x

Huang, J.-G., Bergeron, Y., Denneler, B., Berninger, F., & Tardif, J. (2007). Response of forest trees to increased atmospheric CO_2. *CRC Critical Reviews In Plant Sciences*, *26*(5–6), 265–283. https://doi.org/10.1080/07352680701626978

Hubau, W., Lewis, S. L., Phillips, O. L., Affum-Baffoe, K., Beeckman, H., Cuní-Sanchez, A., et al. (2020). Asynchronous carbon sink saturation in African and Amazonian tropical forests. *Nature*, *579*(7797), 80–87. https://doi.org/10.1038/s41586-020-2035-0

Hülsmann, L., Bugmann, H., Cailleret, M., & Brang, P. (2018). How to kill a tree: Empirical mortality models for 18 species and their performance in a dynamic forest model. *Ecological Applications*, *28*(2), 522–540. https://doi.org/10.1002/eap.1668

Huntzinger, D. N., Michalak, A. M., Schwalm, C., Ciais, P., King, A. W., Fang, Y., et al. (2017). Uncertainty in the response of terrestrial carbon sink to environmental drivers undermines carbon-climate feedback predictions. *Scientific Reports*, *7*(1), 4765. https://doi.org/10.1038/s41598-017-03818-2

Jiang, M., Medlyn, B. E., Drake, J. E., Duursma, R. A., Anderson, I. C., Barton, C. V. M., et al. (2020). The fate of carbon in a mature forest under carbon dioxide enrichment. *Nature*, *580*(7802), 227–231. https://doi.org/10.1038/s41586-020-2128-9

Johnson, D. J., Needham, J., Xu, C., Massoud, E. C., Davies, S. J., Anderson-Teixeira, K. J., et al. (2018). Climate sensitive size-dependent survival in tropical trees. *Nature Ecology & Evolution*, *2*(9), 1436–1442. https://doi.org/10.1038/s41559-018-0626-z

Keeling, R. F., Piper, S. C., & Heimann, M. (1996). Global and hemispheric CO_2 sinks deduced from changes in atmospheric O_2 concentration. *Nature*, *381*(6579), 218–221. https://doi.org/10.1038/381218a0

Körner, C. (2006). Plant CO_2 responses: An issue of definition, time and resource supply. *New Phytologist*, *172*(3), 393–411. https://doi.org/10.1111/j.1469-8137.2006.01886.x

Körner, C. (2009). Responses of humid tropical trees to rising CO_2. *Annual Review of Ecology, Evolution, and Systematics*, *40*(1), 61–79. https://doi.org/10.1146/annurev.ecolsys.110308.120217

Körner, C. (2017). A matter of tree longevity. *Science*, *355*(6321), 130–131. https://doi.org/10.1126/science.aal2449

Kubiske, M. E., Woodall, C. W., & Kern, C. C. (2019). Increasing atmospheric CO_2 concentration stand development in trembling Aspen forests: Are outdated density management guidelines in need of revision for all species? *Journal of Forestry*, *117*(1), 38–45. https://doi.org/10.1093/jofore/fvy058

Kuznetsova, A., Brockhoff, P. B., & Christensen, R. H. B. (2017). lmerTest package: Tests in linear mixed effects models. *Journal of Statistical Software*, *82*(13). https://doi.org/10.18637/jss.v082.i13

Landsberg, J. J., & Waring, R. H. (1997). A generalized model of forest productivity using simplified concepts of radiation-use efficiency, carbon balance and partitioning. *Forest Ecology and Management*, *95*(3), 209–228. https://doi.org/10.1016/s0378-1127(97)00026-1

Leuning, R., Kelliher, F. M., Pury, D. G. G., & Schulze, E.-D. (1995). Leaf nitrogen, photosynthesis, conductance and transpiration: Scaling from leaves to canopies. *Plant, Cell and Environment*, *18*(10), 1183–1200. https://doi.org/10.1111/j.1365-3040.1995.tb00628.x

Lewis, S. L., Lopez-Gonzalez, G., Sonké, B., Affum-Baffoe, K., Baker, T. R., Ojo, L. O., et al. (2009). Increasing carbon storage in intact African tropical forests. *Nature*, *457*(7232), 1003–1006. https://doi.org/10.1038/nature07771

Loehle, C. (1988). Tree life history strategies: The role of defenses. *Canadian Journal of Forest Research*, *18*(2), 209–222. https://doi.org/10.1139/x88-032

Luo, Y., Su, B. O., Currie, W. S., Dukes, J. S., Finzi, A., Hartwig, U., et al. (2004). Progressive nitrogen limitation of ecosystem responses to rising atmospheric carbon dioxide. *BioScience*, *54*(8), 731. https://doi.org/10.1641/0006-3568(2004)054[0731:pnloer]2.0.co;2

Luo, Y., & Weng, E. (2011). Dynamic disequilibrium of the terrestrial carbon cycle under global change. *Trends in Ecology & Evolution*, *26*(2), 96–104. https://doi.org/10.1016/j.tree.2010.11.003

Mäkelä, A., Landsberg, J., Ek, A. R., Burk, T. E., Ter-Mikaelian, M., Agren, G. I., et al. (2000). Process-based models for forest ecosystem management: Current state of the art and challenges for practical implementation. *Tree Physiology*, *20*(5–6), 289–298. https://doi.org/10.1093/treephys/20.5-6.289

Manusch, C., Bugmann, H., Heiri, C., & Wolf, A. (2012). Tree mortality in dynamic vegetation models—A key feature for accurately simulating forest properties. *Ecological Modelling*, *243*, 101–111. https://doi.org/10.1016/j.ecolmodel.2012.06.008

Maschler, J., Bialic-Murphy, L., Wan, J., Andresen, L. C., Zohner, C. M., Reich, P. B., et al. (2022). Links across ecological scales: Plant biomass responses to elevated CO_2. *Global Change Biology*, *28*(21), 6115–6134. https://doi.org/10.1111/gcb.16351

McDowell, N., Allen, C. D., Anderson-Teixeira, K., Brando, P., Brienen, R., Chambers, J., et al. (2018). Drivers and mechanisms of tree mortality in moist tropical forests. *New Phytologist*, *219*(3), 851–869. https://doi.org/10.1111/nph.15027

McDowell, N. G., Allen, C. D., Anderson-Teixeira, K., Aukema, B. H., Bond-Lamberty, B., Chini, L., et al. (2020). Pervasive shifts in forest dynamics in a changing world. *Science*, *368*(6494). https://doi.org/10.1126/science.aaz9463

McDowell, N. G., Beerling, D. J., Breshears, D. D., Fisher, R. A., Raffa, K. F., & Stitt, M. (2011). The interdependence of mechanisms underlying climate-driven vegetation mortality. *Trends in Ecology & Evolution*, *26*(10), 523–532. https://doi.org/10.1016/j.tree.2011.06.003

McDowell, N. G., Sapes, G., Pivovaroff, A., Adams, H. D., Allen, C. D., Anderegg, W. R. L., et al. (2022). Mechanisms of woody-plant mortality under rising drought, CO_2 and vapor pressure deficit. *Nature Reviews Earth & Environment*, *3*(5), 294–308. https://doi.org/10.1038/s43017-022-00272-1

McMahon, S. M., Arellano, G., & Davies, S. J. (2019). The importance and challenges of detecting changes in forest mortality rates. *Ecosphere*, *10*(2), e02615. https://doi.org/10.1002/ecs2.2615

McMahon, S. M., Parker, G. G., & Miller, D. R. (2010). Evidence for a recent increase in forest growth. *Proceedings of the National Academy of Sciences of the United States of America*, *107*(8), 3611–3615. https://doi.org/10.1073/pnas.0912376107

Midgley, J. J. (2001). Do mixed-species mixed-size indigenous forests also follow the self-thinning line? *Trends in Ecology & Evolution*, *16*(12), 661–662. https://doi.org/10.1016/s0169-5347(01)02362-x

Morris, E. C., & Charles Morris, E. (2003). How does fertility of the substrate affect intraspecific competition? Evidence and synthesis from self-thinning. *Ecological Research*, *18*(3), 287–305. https://doi.org/10.1046/j.1440-1703.2003.00555.x

Mrad, A., Manzoni, S., Oren, R., Vico, G., Lindh, M., & Katul, G. (2020). Recovering the metabolic, self-thinning, and constant final yield rules in mono-specific stands. *Frontiers in Forests and Global Change*, *3*. https://doi.org/10.3389/ffgc.2020.00062

Nagel, L. M., Palik, B. J., Battaglia, M. A., D'Amato, A. W., Guldin, J. M., Swanston, C. W., et al. (2017). Adaptive silviculture for climate change: A national experiment in manager-scientist partnerships to apply an adaptation framework. *Journal of Forestry*, *115*(3), 167–178. https://doi.org/10.5849/jof.16-039

Nakagawa, S., & Schielzeth, H. (2013). A general and simple method for obtaining R^2 from generalized linear mixed-effects models. *Methods in Ecology and Evolution*, *4*(2), 133–142. https://doi.org/10.1111/j.2041-210x.2012.00261.x

Needham, J. F., Chambers, J., Fisher, R., Knox, R., & Koven, C. D. (2020). Forest responses to simulated elevated CO_2 under alternate hypotheses of size- and age-dependent mortality. *Global Change Biology*, *26*(10), 5734–5753. https://doi.org/10.1111/gcb.15254

Needham, J. F., Johnson, D. J., Anderson-Teixeira, K. J., Bourg, N., Bunyavejchewin, S., Butt, N., et al. (2022). Demographic composition, not demographic diversity, predicts biomass and turnover across temperate and tropical forests. *Global Change Biology*, *28*(9), 2895–2909. https://doi.org/10.1111/gcb.16100

Needham, J. F., Merow, C., Chang-Yang, C.-H., Caswell, H., & McMahon, S. (2018). Inferring forest fate from demographic data: From vital rates to population dynamic models. *Proceedings of the Royal Society B*, *285*(1874), 20172050. https://doi.org/10.1098/rspb.2017.2050

Norby, R. J., Delucia, E. H., Gielen, B., Calfapietra, C., Giardina, C. P., King, J. S., et al. (2005). Forest response to elevated CO_2 is conserved across a broad range of productivity. *Proceedings of the National Academy of Sciences of the United States of America*, *102*(50), 18052–18056. https://doi.org/10.1073/pnas.0509478102

Norby, R. J., Warre, J. M., Iversen, C. M., Medlyn, B. E., & McMurtrie, R. E. (2010). CO_2 enhancement of forest productivity constrained by limited nitrogen availability. *Proceedings of the National Academy of Sciences of the United States of America*, *107*(45), 19368–19373. https://doi.org/10.1073/pnas.1006463107

Norby, R. J., & Zak, D. R. (2011). Ecological lessons from free-air CO_2 enrichment (FACE) experiments. *Annual Review of Ecology, Evolution and Systematics*, *42*(1), 181–203. https://doi.org/10.1146/annurev-ecolsys-102209-144647

Oksanen, J., Simpson, G., Blanchet, F., Kindt, R., Legendre, P., Minchin, P., et al. (2022). Vegan: Community ecology package. R package version 2.6-4.

Pan, Y., Birdsey, R. A., Fang, J., Houghton, R., Kauppi, P. E., Kurz, W. A., et al. (2011). A large and persistent carbon sink in the world's forests. *Science*, *333*(6045), 988–993. https://doi.org/10.1126/science.1201609

Phillips, O. L., Aragão, L. E. O. C., Lewis, S. L., Fisher, J. B., Lloyd, J., López-González, G., et al. (2009). Drought sensitivity of the Amazon rainforest. *Science*, *323*(5919), 1344–1347. https://doi.org/10.1126/science.1164033

Piao, S., Liu, Q., Chen, A., Janssens, I. A., Fu, Y., Dai, J., et al. (2019). Plant phenology and global climate change: Current progresses and challenges. *Global Change Biology*, *25*(6), 1922–1940. https://doi.org/10.1111/gcb.14619

Portier, J., Wunder, J., Stadelmann, G., Zell, J., Abegg, M., Thürig, E., & Rohner, B. (2021). "Latent reserves": A hidden treasure in national forest inventories. *Journal of Ecology*, *109*(1), 369–383. https://doi.org/10.1111/1365-2745.13487

Pretzsch, H. (2006). Species-specific allometric scaling under self-thinning: Evidence from long-term plots in forest stands. *Oecologia*, *146*(4), 572–583. https://doi.org/10.1007/s00442-005-0126-0

Pretzsch, H., Biber, P., Schütze, G., Uhl, E., & Rötzer, T. (2014). Forest stand growth dynamics in Central Europe have accelerated since 1870. *Nature Communications*, *5*(1), 4967. https://doi.org/10.1038/ncomms5967

Pugh, T. A. M., Rademacher, T., Shafer, S. L., Steinkamp, J., Barichivich, J., Beckage, B., et al. (2020). Understanding the uncertainty in global forest carbon turnover. *Biogeosciences*, *17*(15), 3961–3989. https://doi.org/10.5194/bg-17-3961-2020

Purves, D. W., Lichstein, J. W., & Pacala, S. W. (2007). Crown plasticity and competition for canopy space: A new spatially implicit model parameterized for 250 North American tree species. *PLoS One*, *12*(9), e870. https://doi.org/10.1371/journal.pone.0000870

Purves, D. W., Lichstein, J. W., Strigul, N., & Pacala, S. W. (2008). Predicting and understanding forest dynamics using a simple tractable model. *Proceedings of the National Academy of Sciences of the United States of America*, *105*(44), 17018–17022. https://doi.org/10.1073/pnas.0807754105

Randerson, J. T., Thompson, M. V., Conway, T. J., Fung, I. Y., & Field, C. B. (1997). The contribution of terrestrial sources and sinks to trends in the seasonal cycle of atmospheric carbon dioxide. *Global Biogeochemical Cycles*, *11*(4), 535–560. https://doi.org/10.1029/97gb02268

R Core Team. (2021). *R: A language and environment for statistical computing*. R Foundation for Statistical Computing. Retrieved from https://www.R-project.org/

Reineke, L. H. (1933). Perfecting a stand-density index for even-aged forests. *Journal of Agricultural Research*, *46*, 627–638.

Reyes-Hernandez, V., Comeau, P. G., & Bokalo, M. (2013). Static and dynamic maximum size–density relationships for mixed trembling aspen and white spruce stands in western Canada. *Forest Ecology and Management*, *289*, 300–311. https://doi.org/10.1016/j.foreco.2012.09.042

Rivoire, M., & Le Moguedec, G. (2012). A generalized self-thinning relationship for multi-species and mixed-size forests. *Annals of Forest Science*, *69*(2), 207–219. https://doi.org/10.1007/s13595-011-0158-z

Schwalm, C. R., Anderegg, W. R. L., Michalak, A. M., Fisher, J. B., Biondi, F., Koch, G., et al. (2017). Global patterns of drought recovery. *Nature*, *548*(7666), 202–205. https://doi.org/10.1038/nature23021

Senf, C., Pflugmacher, D., Zhiqiang, Y., Sebald, J., Knorn, J., Neumann, M., et al. (2018). Canopy mortality has doubled in Europe's temperate forests over the last three decades. *Nature Communications*, *9*(1), 4978. https://doi.org/10.1038/s41467-018-07539-6

Sitch, S., Smith, B., Prentice, I. C., Arneth, A., Bondeau, A., Cramer, W., et al. (2003). Evaluation of ecosystem dynamics, plant geography and terrestrial carbon cycling in the LPJ dynamic global vegetation model. *Global Change Biology*, *9*(2), 161–185. https://doi.org/10.1046/j.1365-2486.2003.00569.x

Smith, A. R., Lukac, M., Bambrick, M., Miglietta, F., & Godbold, D. L. (2013). Tree species diversity interacts with elevated CO_2 to induce a greater root system response. *Global Change Biology*, *19*(1), 217–228. https://doi.org/10.1111/gcb.12039

Sommerfeld, A., Senf, C., Buma, B., D'Amato, A. W., Després, T., Díaz-Hormazábal, I., et al. (2018). Patterns and drivers of recent disturbances across the temperate forest biome. *Nature Communications*, *9*(1), 4355. https://doi.org/10.1038/s41467-018-06788-9

Song, J., Wan, S., Piao, S., Knapp, A. K., Classen, A. T., Vicca, S., et al. (2019). A meta-analysis of 1,119 manipulative experiments on terrestrial carbon-cycling responses to global change. *Nature Ecology & Evolution*, *3*(9), 1309–1320. https://doi.org/10.1038/s41559-019-0958-3

Stocker, B., Marqués, L., & Hufkens, K. (2021). *rsofun v4.0 Modelling framework for site-scale simulations of ecosystem processes in R (v4.0)*. Zenodo.

Terrer, C., Jackson, R. B., Prentice, I. C., Keenan, T. F., Kaiser, C., Vicca, S., et al. (2019). Nitrogen and phosphorus constrain the CO_2 fertilization of global plant biomass. *Nature Climate Change*, *9*, 684–689. https://doi.org/10.1038/s41558-019-0545-2

Terrer, C., Vicca, S., Stocker, B. D., Hungate, B. A., Phillips, R. P., Reich, P. B., et al. (2018). Ecosystem responses to elevated CO_2 governed by plant–soil interactions and the cost of nitrogen acquisition. *New Phytologist*, *217*(2), 507–522. https://doi.org/10.1111/nph.14872

Vicca, S., Luyssaert, S., Peñuelas, J., Campioli, M., Chapin, F. S., III., Ciais, P., et al. (2012). Fertile forests produce biomass more efficiently. *Ecology Letters*, *15*(6), 520–526. https://doi.org/10.1111/j.1461-0248.2012.01775.x

Walker, A. P., De Kauwe, M. G., Bastos, A., Belmecheri, S., Georgiou, K., Keeling, R. F., et al. (2021). Integrating the evidence for a terrestrial carbon sink caused by increasing atmospheric CO. *New Phytologist*, *229*(5), 2413–2445. https://doi.org/10.1111/nph.16866

Walker, A. P., De Kauwe, M. G., Medlyn, B. E., Zaehle, S., Iversen, C. M., Asao, S., et al. (2019). Decadal biomass increment in early secondary succession woody ecosystems is increased by CO_2 enrichment. *Nature Communications*, *10*, 454. https://doi.org/10.1038/s41467-019-08348-1

Wang, J. A., Baccini, A., Farina, M., Randerson, J. T., & Friedl, M. A. (2021). Disturbance suppresses the aboveground carbon sink in North American boreal forests. *Nature Climate Change*, *11*(5), 435–441. https://doi.org/10.1038/s41558-021-01027-4

Weiskittel, A. R., Temesgen, H., Wilson, D. S., & Maguire, D. A. (2008). Sources of within- and between-stand variability in specific leaf area of three ecologically distinct conifer species. *Annals of Forest Science*, *65*(1), 103. https://doi.org/10.1051/forest:2007075

Weng, E., Dybzinski, R., Farrior, C. E., & Pacala, S. W. (2019). Competition alters predicted forest carbon cycle responses to nitrogen availability and elevated CO_2: Simulations using an explicitly competitive, game-theoretic vegetation demographic model. *Biogeosciences*, *16*, 4577–4599. https://doi.org/10.5194/bg-16-4577-2019

Weng, E., Farrior, C. E., Dybzinski, R., & Pacala, S. W. (2017). Predicting vegetation type through physiological and environmental interactions with leaf traits: Evergreen and deciduous forests in an Earth system modeling framework. *Global Change Biology*, *23*(6), 2482–2498. https://doi.org/10.1111/gcb.13542

Weng, E. S., Malyshev, S., Lichstein, J. W., Farrior, C. E., Dybzinski, R., Zhang, T., et al. (2015). Scaling from individual trees to forests in an Earth system modeling framework using a mathematically tractable model of height-structured competition. *Biogeosciences*, *12*(9), 2655–2694. https://doi.org/10.5194/bg-12-2655-2015

West, G. B., Brown, J. H., & Enquist, B. J. (1997). A general model for the origin of allometric scaling laws in biology. *Science*, *276*(5309), 122–126. https://doi.org/10.1126/science.276.5309.122

Westoby, M. (1984). The self-thinning rule. In *Advances in ecological research* (pp. 167–225). Elsevier. https://doi.org/10.1016/S0065-2504(08)60171-3

Wood, S. N. (2017). *Generalized additive models: An introduction with R* (2nd ed.). CRC Press. https://doi.org/10.1201/9781315370279

Wright, S. J., Kitajima, K., Kraft, N. J. B., Reich, P. B., Wright, I. J., Bunker, D. E., et al. (2010). Functional traits and the growth-mortality tradeoff in tropical trees. *Ecology*, *91*(12), 3664–3674. https://doi.org/10.1890/09-2335.1

Wu, C., Hember, R. A., Chen, J. M., Kurz, W. A., Price, D. T., Boisvenue, C., et al. (2014). Accelerating forest growth enhancement due to climate and atmospheric changes in British Colombia, Canada over 1956-2001. *Scientific Reports*, *4*(1), 4461. https://doi.org/10.1038/srep04461

Xia, J., Luo, Y., Wang, Y.-P., & Hararuk, O. (2013). Traceable components of terrestrial carbon storage capacity in biogeochemical models. *Global Change Biology*, *19*(7), 2104–2116. https://doi.org/10.1111/gcb.12172

Yoda, K., Kira, T., Ogawa, H., & Hozumi, K. (1963). Self-thinning in overcrowded pure stands under cultivated and natural conditions. *Journal of Biology*, *14*, 107–129.

Yu, K., Smith, W. K., Trugman, A. T., Condit, R., Hubbell, S. P., Sardans, J., et al. (2019). Pervasive decreases in living vegetation carbon turnover time across forest climate zones. *Proceedings of the National Academy of Sciences of the United States of America*, *116*(49), 24662–24667. https://doi.org/10.1073/pnas.1821387116

Yuan, W., Zheng, Y., Piao, S., Ciais, P., Lombardozzi, D., Wang, Y., et al. (2019). Increased atmospheric vapor pressure deficit reduces global vegetation growth. *Science Advances*, *5*(8), eaax1396. https://doi.org/10.1126/sciadv.aax1396

Zeide, B. (1993). Primary unit of the tree crown. *Ecology*, *74*(5), 1598–1602. https://doi.org/10.2307/1940088

Zuur, A. F., Ieno, E. N., Walker, N., Saveliev, A. A., & Smith, G. M. (2009). *Mixed effects models and extensions in ecology with R. Statistics for Biology and Health*. Springer.

References From the Supporting Information

Myneni, R., Knyazikhin, Y., & Park, T. (2015). MCD15A3H MODIS/Terra+Aqua Leaf Area Index/FPAR 4-day L4 Global 500m SIN Grid V006. NASA EOSDIS Land Processes DAAC. http://doi.org/10.5067/MODIS/MCD15A3H.006

Pastorello, G., Trotta, C., Canfora, E., Chu, H., Christianson, D., Cheah, Y.-W., et al. (2020). The FLUXNET2015 dataset and the ONEFlux processing pipeline for eddy covariance data. *Scientific Data*, *7*(1), 225. https://doi.org/10.1038/s41597-020-0534-3

Thimonier, A., Graf Pannatier, E., Schmitt, M., Waldner, P., Walthert, L., Schleppi, P., et al. (2010). Does exceeding the critical loads for nitrogen alter nitrate leaching, the nutrient status of trees and their crown condition at Swiss Long-term Forest Ecosystem Research (LWF) sites? *European Journal of Forest Research*, *129*(3), 443–461. https://doi.org/10.1007/s10342-009-0328-9

Xiang, Y., Gubian, S., Suomela, B., & Hoeng, J. (2013). Generalized simulated annealing for global optimization: The GenSA package. *R J*, *5*(1), 13. https://doi.org/10.32614/rj-2013-002